STUDY OF A SMALL SOLAR PROBE

(Sunblazer)

7-1-64 to 6-30-65

Part I

RADIO PROPAGATION EXPERIMENT

by

J. V. Harrington

PR-5255-5 July 1, 1965

MASSACHUSETTS INSTITUTE OF TECHNOLOGY

CENTER FOR SPACE RESEARCH

STUDY OF A SMALL SOLAR PROBE

(Sunblazer)

Part I. Radio Propagation Experiment

by

J. V. Harrington

July 1, 1965

Work done under

NATIONAL AERONAUTICS AND SPACE ADMINISTRATION

GRANT NASr-249

STUDY OF A SMALL SOLAR PROBE

(Sunblazer)

This report is intended to summarize the work done during the period June 1964 to June 1965 on the Sunblazer project.

I. Principal Objectives of The Study

The central purpose of the study was to determine the feasibility of measuring the electron density and other features of the solar corona using a radio propagation method based on the observation of coherent multifrequency transmissions from a small heliocentric orbiting satellite which achieves superior conjunction in one year. The study was to determine, from plausible models of the coronal density and structure, what the effect would be on signals propagated through the corona, on paths displaced by varying amounts from the photosphere. The quantities to be calculated included the relative delay, the expected variations in angle of arrival of the signals at a terrestrial antenna, the rotation of the plane of polarization, and any absorption or attenuation effects. Conversely, having computed these observables, the extent to which their measurements might reveal interesting properties of the corona was to be examined. While the major scientific objectives were (a) the determination of the coronal electron density profile in the range from three solar radii to 100 solar radii, it was also hoped that (b) Faraday rotation measurements or direct observations of ordinary-extraordinary

mode propagation would reveal some of the gross features of the sun's general magnetic field, and (c) that the simultaneous observations of the angle of arrival fluctuation and path length or delay fluctuations, made possible by employing coherent transmissions, would lead to a unique determination of the scale size of the density fluctuations in the inner corona.

Associated with these scientific investigations was the design of the solar orbiting spacecraft and its payload. The objective was to make the spacecraft a simple one containing little more than a power supply, a multifrequency transmitter, and omni-directional antennas. It was believed that the functional simplicity of the spacecraft would lead to a very low weight (ten pounds was our design objective) such that relatively low-cost launch vehicles could boost the spacecraft to the necessary high (about 40,000 feet per second) launch velocities. The further hope was that an unguided launch vehicle could be employed in view of the wide variation ($\pm$ 20°) in orientation that the vehicle's excess velocity vector may have after terrestrial escape and still be injected into a useful heliocentric orbit. It was believed that the use of both light-weight spacecraft and unguided solid-propellant launch vehicles would make it economically attractive to launch several such spacecraft per year so that systematic measurements of the coronal electron density profile, which is known to fluctuate markedly with solar activity, could be made.

II. Principal Conclusions

For reasonable models [Baumbach, 1937; van de Hulst, 1950; Erickson, 1964; Brandt, 1964] of the electron density distribution in the corona, the relative delay between signals transmitted on frequencies of 100 and 300 MC on very long (> 2 A.U.) paths displaced from the solar center from two solar radii to 100 solar radii varies from $\sim$ 100 ms (10^{18} electrons per cm^2) to 300 μs (2×10^{15} electrons/cm^2) and are readily measurable. The accuracy of the measurement may be of the order of 20 μs (10^{14} electrons per cm^2) or better, and the uncertainty produced by the earth's ionosphere is about 1 μs (10^{13} electrons/cm^2). Analyses indicate that the densities between 40 to 100 $r_\odot$ would be measured as averages over a two-month period; the densities in the interval between 10 to 40 solar radii would represent 12-day averages; and for the interval between 2 to 10 $r_\odot$, the averaging would be over the three-day period just prior to superior conjunction. Given sufficient satellite lifetime, the measurements may be repeated in the time period beyond conjunction.

The most desirable heliocentric orbit to employ is one with perihelion at 0.53 A.U. and a sidereal period of 0.667 years [Harrington, 1964]. This permits conjunction to occur in one year on the line of apses and gives a mirror symmetry of the transmission path before and after conjunction. The measurement of the angular scintillation and fluctuation in time of arrival of signals on the 100 MC carrier offers a good possibility for uniquely determining the scale size of the scattering inhomogene-

ities when the path is displaced by a few solar radii from the photosphere. In this region, the scintillation spectrum will have a width of from six to 18 minutes of arc, and the corresponding fluctuations in signal time of arrival would be of the order of 25 to 75 μs and should be observable.

Pulse splitting produced by ordinary-extraordinary mode propagation offers the best opportunity to make quantitative measurements of the general magnetic field of the sun. For one very elementary model of the general magnetic field, it was concluded that the magnetoionic effects produced by the corona will not dominate those produced by the terrestrial ionosphere until the path displacement is less than 10 solar radii. While detailed information on the general solar field is not likely to be obtained from Faraday rotation and pulse-splitting observations, rather useful information on the gross features of the general magnetic field in the inner corona ($r_{\odot} < 10$) will be obtained.

The feasibility of designing a spacecraft containing within the stringent weight limitations the necessary power supply, transmitters, and antennas has been demonstrated by the construction of a full-size working model. The spacecraft is designed to be radially stabilized by solar radiation pressure, employs a solar cell array to provide 12 watts of power at 1 A.U. and 30 watts at 0.5 A.U., has transmitters capable of delivering 500 watts of peak power at 100 and 300 MC, does not require any active temperature control even at 0.5 A.U., has no erectable booms or structures except for simple whip antennas, and weighs a total of 13.8 pounds.

III. Radio Propagation Experiments

A. The Electron Density in the Solar Corona

The first quantitative description of the electron density profile in the solar corona comes from the work of Baumbach [1937] who determined an average electron density profile from a study of the brightness distribution in the corona as observed at the time of a solar eclipse. The method depends upon a knowledge of the mechanism whereby white light is scattered from the free electrons in the corona. Baumbach's results were further improved by Allen [1947] and van de Hulst [1950] to obtain the well-known Allen-Baumbach relation:

$$N(r) = 10^8 \left[\frac{1.55}{r^6} + \frac{2.99}{r^{16}}\right] \text{ electrons/cc} \qquad [1]$$

where r is in solar radii. This expression provides a good description of the average coronal electron density near solar maximum. Since the coronal brightness is only readily measurable out to a few solar radii, the light-scattering method can only reveal the electron density distribution for $r_\odot < 5$.

An occultation method has come into use over the past decade which establishes the existence of appreciable electron densities out to 50 solar radii and, in one instance, as far as 100 solar radii. The method has been widely used and involves the observation of radio stars as they are occulted by the solar corona [Vitkevich, 1959; Hewish, 1955, 1958, 1963; Slee, 1961; Högbom, 1960; Erickson, 1964]. From the amount of angular scattering as measured by very narrow-beam interferometers operating at metric

wavelengths, indirect information on the coronal electron densities can be determined. The method is indirect in the sense that the measured scintillation determines only the ratio of the rms density fluctuation to the scale size of the scattering inhomogeneities [Hewish, 1955; Fejer, 1953, Chandrasekar, 1952] so that a unique measurement of interplanetary electron density is not possible. By assuming a linear relationship between the density fluctuations and the average density, the variation of average density with distance from the sun can be inferred [Högbom, 1960; Erickson, 1964].

A third method for determining interplanetary particle densities and the first direct method has been made possible with instruments aboard interplanetary probes. Direct measurements of the interplanetary plasma [Bridge, 1964] have given accurate data but only in the vicinity of the earth for $r_\Theta \approx 215$ where densities of the order of 10 electrons/cc have been observed.

Thus the situation as far as one of the fundamental quantities in the extended corona is concerned is somewhat unsettled. Except for the few direct measurements made at 200 solar radii, all of the other measurements are indirect, and of these only the measurements within five solar radii are unambiguous and reliable. There is a gap from five to 50 solar radii only partially explored by radio wave-scattering measurements and a great gap from 50 to 200 solar radii in which almost no data exist. A method which will give a continuous profile from three solar radii out to 100 solar radii would fill a need and its use becomes attractive. The

method is based on observing the delay of signals transmitted on several frequencies from a solar orbiting spacecraft to a terrestrial receiver. The differential delay between signals on the separate carriers provides a direct measure of the integrated electron densities along the transmission paths. The observation of the columnar densities on a large number of paths penetrating more deeply into the corona near occultation then permits the radial electron density distribution to be computed.

There is considerable evidence [Brandt, 1965; Erickson, 1964] that the coronal electron density profile fluctuates markedly with the activity of the sun with the densities in the outer regions at solar maximum greater by a factor of 10 or more than the densities at solar minimum. Similarly, electron densities in coronal streamers or in regions of the corona above flares can be an order of magnitude greater than the Allen-Baumbach densities in the lower corona [Wild, 1959]. For analysis purposes throughout the study, the Allen-Baumbach expression was used, augmented by an inverse second power term which fits the data measured by direct probe at one A.U. In the region beyond 1.5 solar radii, the inverse 16th power term in the Allen-Baumbach expression may be neglected, giving a simple expression for the average electron density in the extended corona of:

$$N(r) \approx \frac{10^8}{r^6} + \frac{10^6}{r^2}; \quad r_\odot > 1.5 \qquad [2]$$

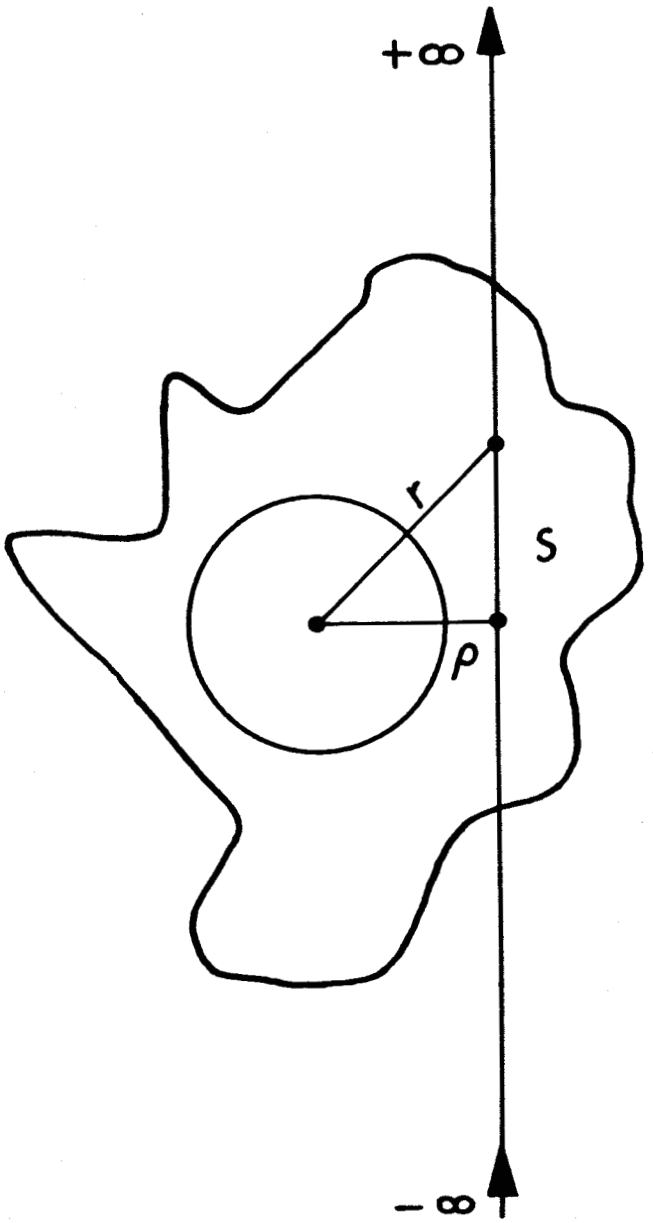

ρ - path offset

FIGURE 1. Transmission path through corona

This is the expression used for the delay calculations of Figures 4 and 5 and probably leads to estimates for delay that are median estimates. At times of greater solar activity, the densities and delays may be an order of magnitude larger.

B. Analytical Relations between Columnar and Radial Densities

The relative delay of signals propagated along an infinite path displaced from the solar center by a distance ρ (Figure 1) measures the columnar densities or the total number of electrons contained in a unit cross section integrated along the entire path. If the electron density is a function only of the radial distance from the sun, i.e. the electron density exhibits cylindrical symmetry in the plane containing the transmission path and the solar center, which in our case would normally be the plane of the ecliptic, then the columnar and radial densities are related by the simple integral:

$$T(\rho) = \int_{-\infty}^{\infty} N(R)\ dS = R_o \int_{-\infty}^{\infty} N\ (r)\ ds \qquad [3]$$

where lower case distances have been normalized with respect to the solar radius, R_o. By expressing the distances along the path in terms of r and ρ, since $r^2 = s^2 + \rho^2$, we find:

$$T(\rho) = 2\ R_o \int_{\rho}^{\infty} \frac{N(r)\ r\ dr}{\sqrt{r^2 - \rho^2}} \qquad [4]$$

This is an Abel integral equation, and similar equations occur [Baumbach, 1937; van de Hulst, 1950] in the calculation of the

intensity of visible light scattered from the coronal electrons. Fortunately, the equation has a unique solution such that:

$$N(r) = - \frac{1}{R_o \pi} \frac{d}{dr} \int_r^\infty \frac{r}{\rho} \frac{T(\rho)\, d\rho}{\sqrt{\rho^2 - r^2}} \qquad [5]$$

In mathematical terms N (r) and T(ρ) are Abel transforms of one another. A measurement of one determines the other, and vice versa. Thus, if T(ρ) can be determined over some range of path displacements, the radial densities can be uniquely determined over the same range within limits imposed by the assumptions of cylindrical symmetry. When N(r) is expressed as a polynomial in inverse powers of (r) as the physical situation suggests, then a corresponding polynomial for T(ρ) is obtained having the very useful property that its coefficients are related to the a_k by a constant multiplier. Given that:

$$N(r) = \sum_{k=2}^{\infty} \frac{a_k}{r^k} \qquad [6]$$

then:

$$T(\rho) = R_o \sum_{k=2}^{\infty} \frac{c_k\, a_k}{\rho^{k-1}} \qquad [7]$$

where $c_2 = \pi$, $c_3 = 2$, $c_4 = \frac{\pi}{2}$, $c_5 = \frac{4}{3}$, $c_6 = \frac{3\pi}{8}$, and the remainder can be calculated from the generating function:

$$c_k = \left(\frac{k-3}{k-2}\right) c_{k-2} \qquad [8]$$

For

$$N(r) = \frac{10^8}{r^6} + \frac{10^6}{r^2} \text{ electrons/cm}^3 \qquad [9]$$

then the corresponding expression for the columnar density is:

$$T(\rho) = \left[\frac{\frac{3\pi}{8}\,10^8}{\rho^5} + \frac{10^6}{\rho}\right] R_o \text{ electrons/cm}^2 \qquad [10]$$

$$= \left[\frac{8.2 \cdot 10^{18}}{\rho^5} + \frac{2.2 \cdot 10^{17}}{\rho}\right] \text{electrons/cm}^2 \qquad [11]$$

C. Orbital Considerations

The selection of a heliocentric orbit for the delay experiment is determined by the desire to make the time to superior conjunction as short as possible consistent with the requirement that the path terminal should be well outside the dense regions of the corona and consistent with practical limitations imposed by the burnout velocities achievable with reasonable launch vehicles (shorter times to conjunction will be achieved with the higher launch velocities, but perihelion will be closer to the sun). An additional factor is the desire to obtain symmetry in the transmission path geometry before and after conjunction so that two closely spaced opportunities to make the same delay measurements will be afforded per launch.

In an earlier study [Harrington, 1964] it was shown that the condition for symmetry is met when conjunction falls on the line of apses of the satellite's orbit. A number of launch possibilities exist for achieving this (Table I).

The second of these, which permits conjunction to occur in one year with the satellite at 0.53 A.U. perihelion and requiring a launch velocity of 39.4 Kft per second, is believed to be the

TABLE I. Characteristics of First Few (n = 1) Orbits Producing Desired Summetry

Retrograde Injection

m	Satellite Period t_s	Time to Conjunction t_π	Perihelion r_p	Excess Velocity Δv	Burnout Velocity at 10^6 ft. v_b
1	0.50 yrs.	0.5 yrs.	0.26 A.U.	35.0 K ft/sec.	49.7 K ft/sec.
2*	0.67	1.0	0.53	16.4	39.4
3	0.75	1.5	0.648	11.1	37.4
4	0.80	2.0	0.724	8.3	36.8

* Recommended for Sunblazer

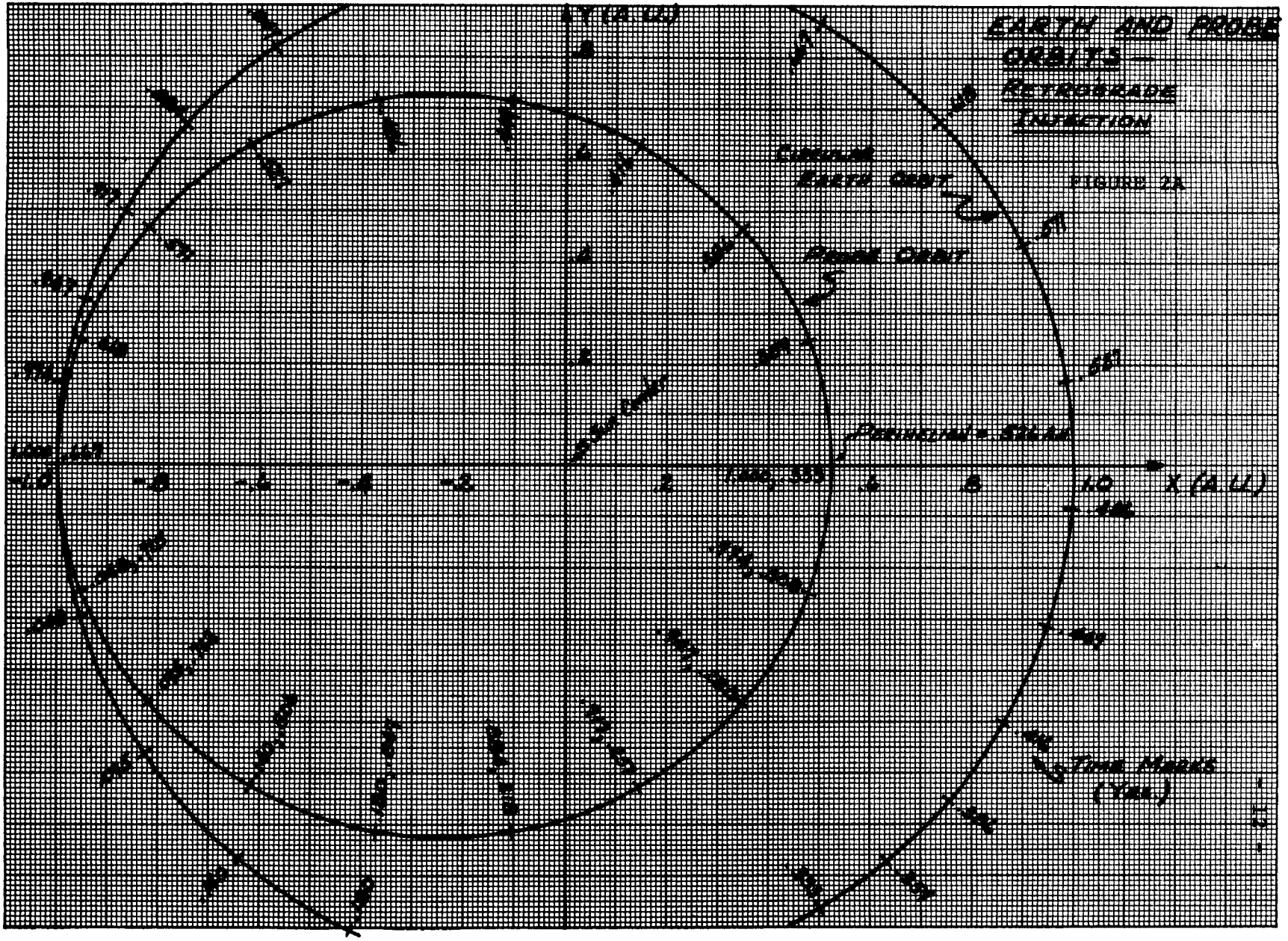
EARTH AND PROBE ORBITS — RETROGRADE INJECTION
FIGURE 2A
CIRCULAR EARTH ORBIT
PROBE ORBIT
PERIHELION = .526 AU
X (A.U.)
Y (A.U.)
TIME MARKS (YRS.)

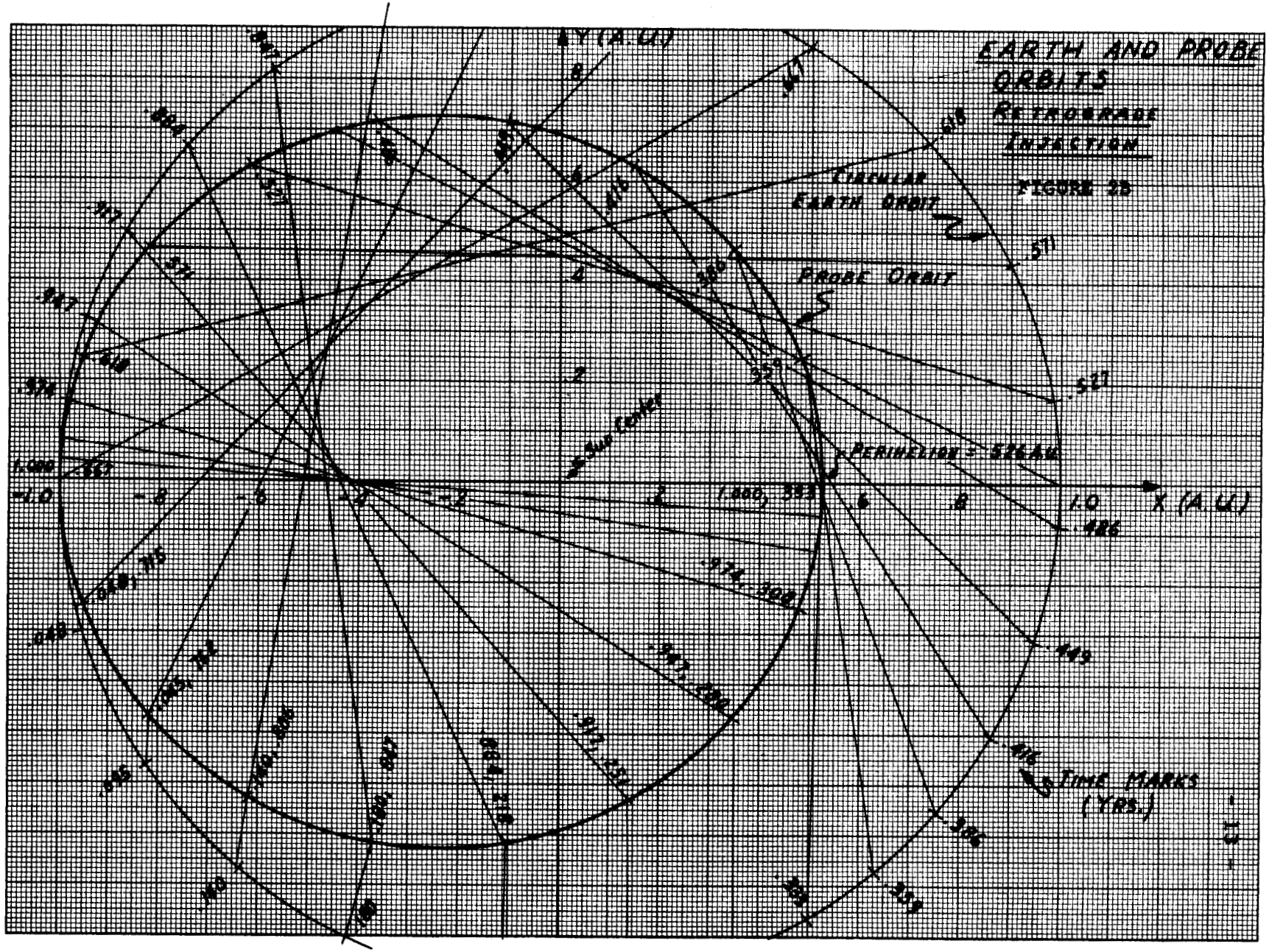
EARTH AND PROBE ORBITS
RETROGRADE INJECTION
FIGURE 25
Y (A.U.)
X (A.U.)
CIRCULAR EARTH ORBIT
PROBE ORBIT
PERIHELION = .526 A.U.
TIME MARKS (YRS.)

PATH OFFSET AND EARTH-PROBE RANGE

RETROGRADE INJECTION

FIGURE 3

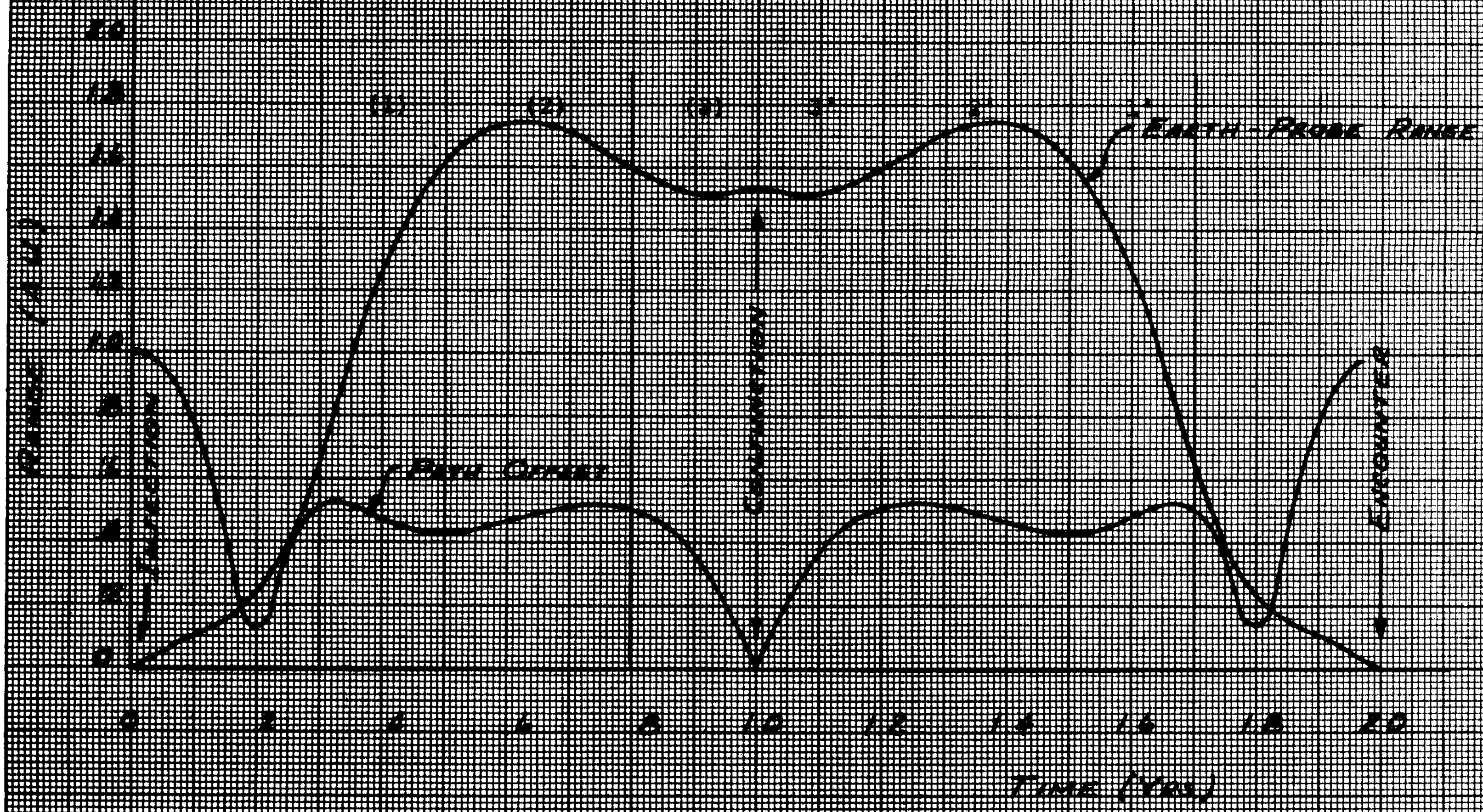

FIGURE 4

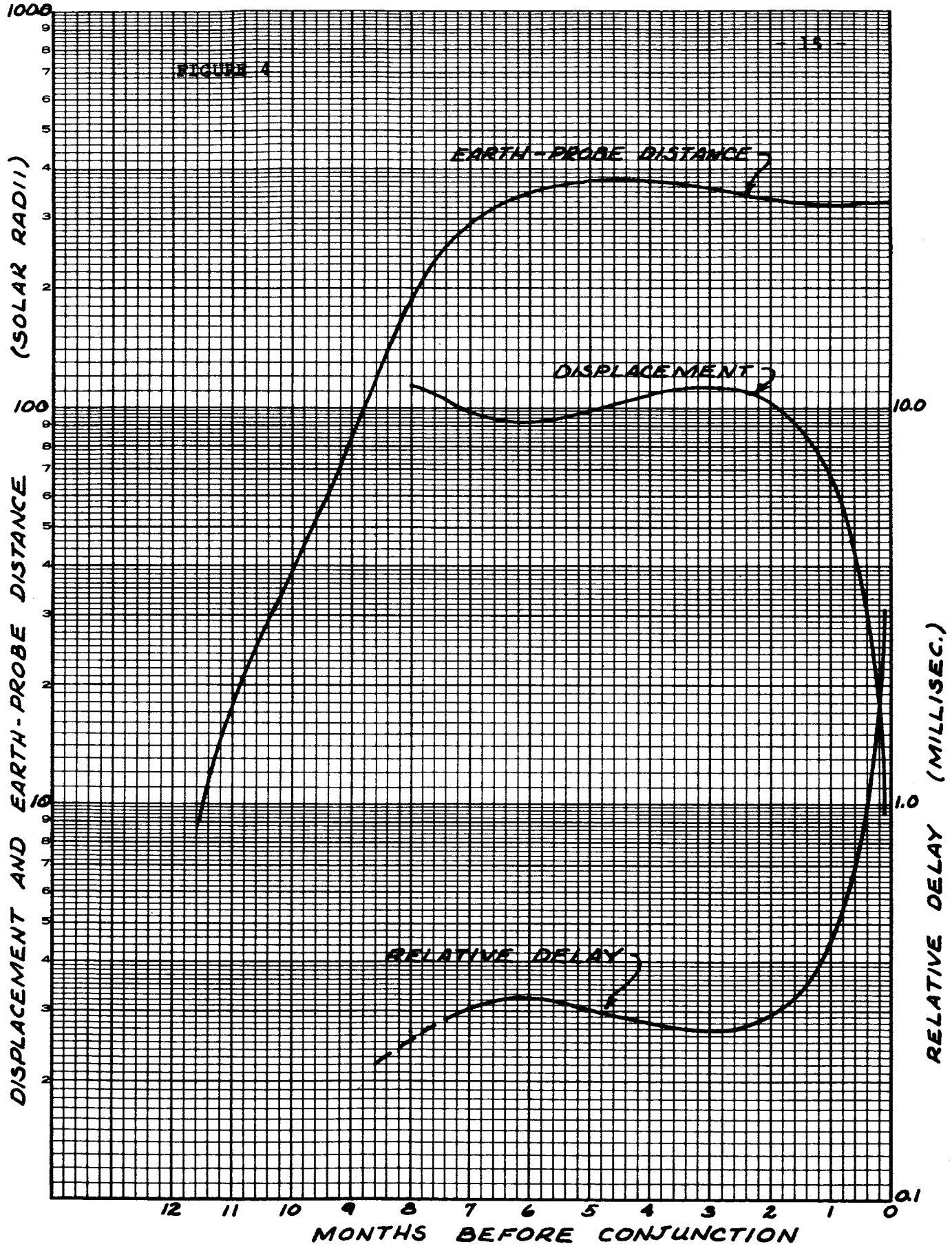
EARTH-PROBE DISTANCE
DISPLACEMENT
RELATIVE DELAY
DISPLACEMENT AND EARTH-PROBE DISTANCE (SOLAR RADII)
RELATIVE DELAY (MILLISEC.)
MONTHS BEFORE CONJUNCTION
1000
100
10
10.0
1.0
0.1
12 11 10 9 8 7 6 5 4 3 2 1 0

FIGURE 5

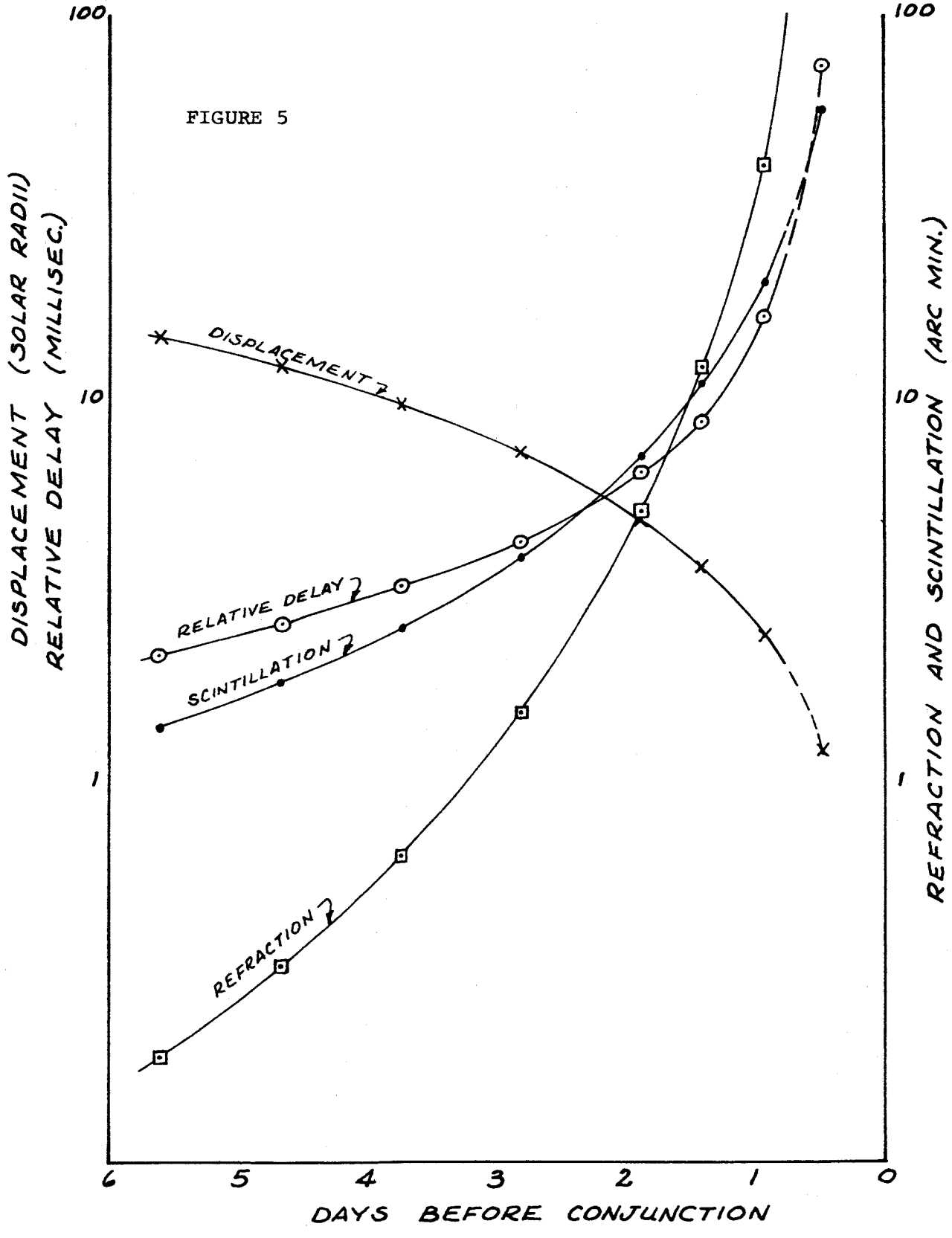
100
10
1
100
10
1
DISPLACEMENT (SOLAR RADII)
RELATIVE DELAY (MILLISEC.)
REFRACTION AND SCINTILLATION (ARC MIN.)
DISPLACEMENT
RELATIVE DELAY
SCINTILLATION
REFRACTION
6
5
4
3
2
1
0
DAYS BEFORE CONJUNCTION

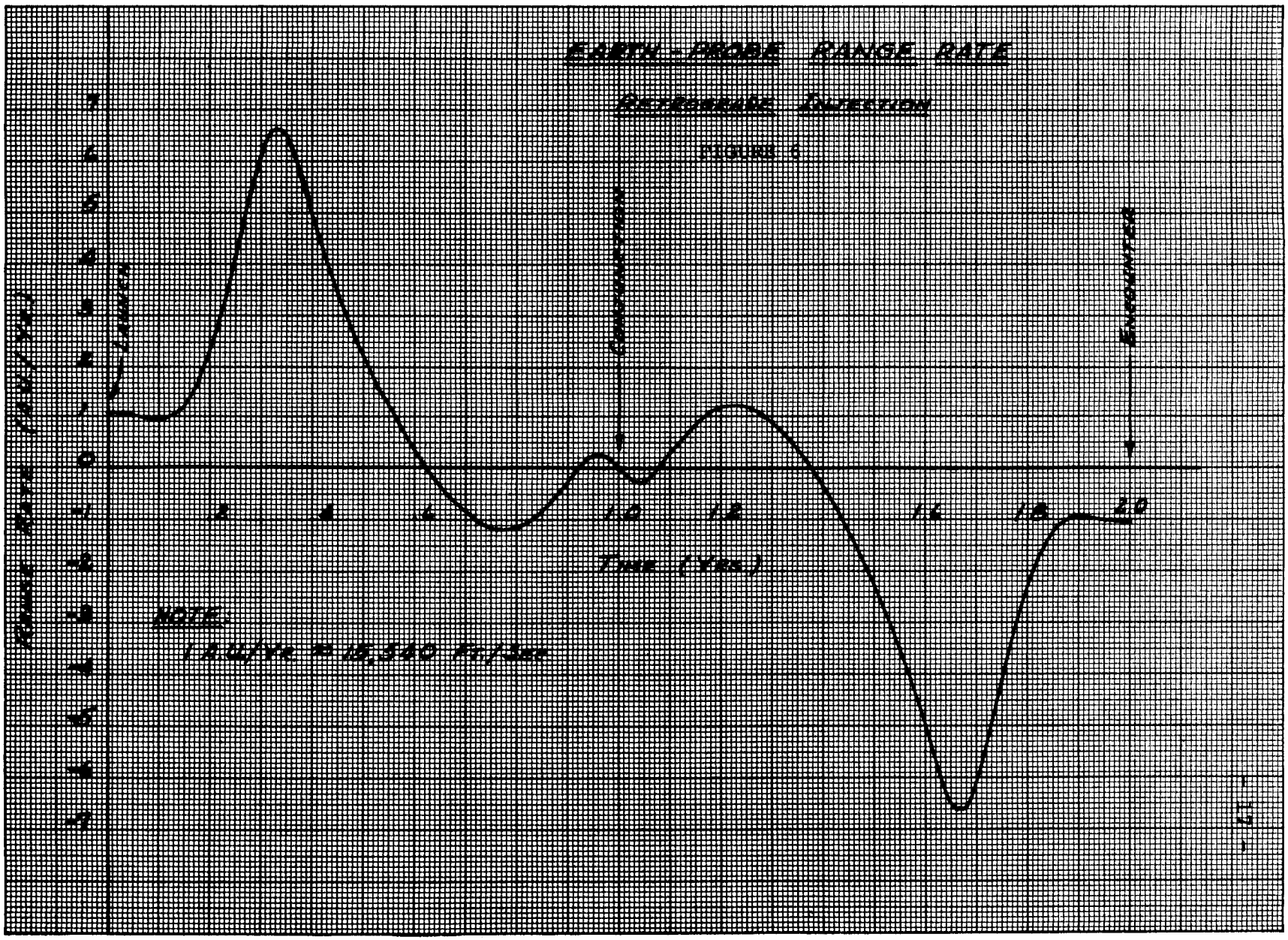
EARTH-PROBE RANGE RATE
RECEDING DIRECTION
FIGURE 6
RANGE RATE (KM/SEC)
7
6
5
4
3
2
1
0
-1
-2
-3
-4
-5
-6
-7
2
4
6
8
10
12
14
16
18
20
TIME (HRS.)
ECLIPSE
NOTE:
1 KM/SEC = 15,540 FT/SEC

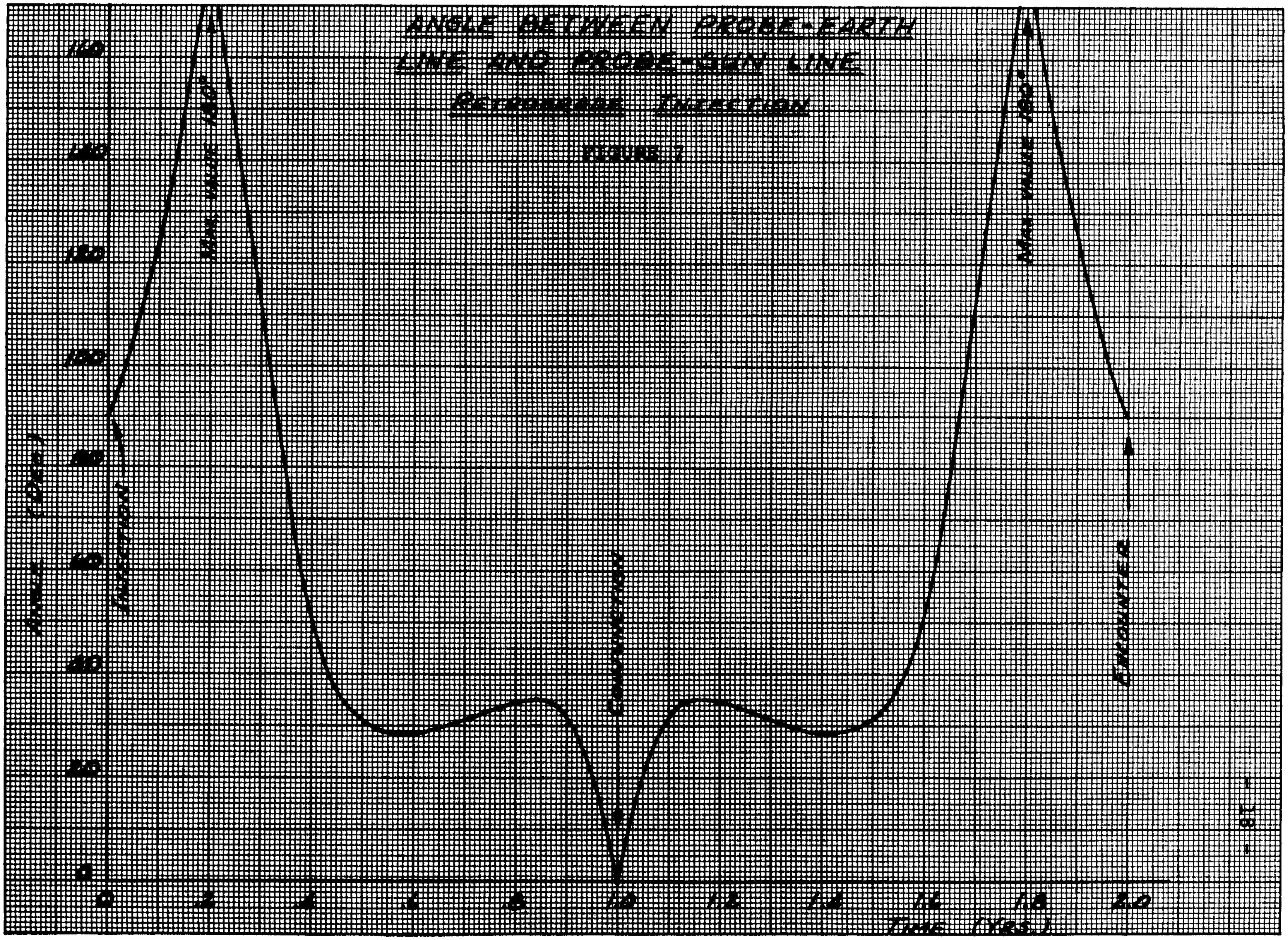
ANGLE BETWEEN PROBE-EARTH
LINE AND PROBE-SUN LINE
RETROGRADE INJECTION
FIGURE 7
ANGLE (DEG.)
160
140
120
100
80
60
40
20
0
0
.2
.4
.6
.8
1.0
1.2
1.4
1.6
1.8
2.0
TIME (YRS.)
INJECTION
MAX. VALUE 180°
CONJUNCTION
MAX. VALUE 180°
ENCOUNTER

most desirable orbit to employ. The earth-satellite transmission path geometry is illustrated in Figure 2. It is evident that in the first half-period of the satellite the direction of the transmission path is fixed approximately radially as the path length increases to about one A.U. In the second half-period, the length is relatively fixed and the path simply rotates about the sun as the satellite's angular velocity and the earth's angular velocity become comparable. Finally, in the third half-period as the satellite passes for the second time through perihelion, the path length remains fixed but the displacement from the solar center is reduced to zero as conjunction occurs. The variation of path length and displacement with time is better illustrated in Figure 3 where the three regions as well as the symmetry before and after conjunction are quite evident.

In region 1 where the path length is growing in an approximately radial direction, the increasing delays can be attributed to the electrons being added at the extremity of the path, and estimates of the interplanetary electron densities in the region from 0.5 A.U. to 1.0 A.U. may be obtained.

In region 2 where both the displacement and the path length are fixed but the angular position of the path is changing by more than 100°, opportunities exist for measuring the extent to which the electron density distribution in the ecliptic exhibits cylindrical symmetry. Observations of delay for fixed path length and fixed displacement may be made over three solar rotations.

In region 3, which is perhaps the most important for our purposes, the path length is fixed at roughly 1.5 A.U. and the displacement decreases monotonically from 0.5 A.U. to zero over a two-month period. The relative delay (Figure 4) is fixed at 300 ms until approximately two months before conjunction and then increased rapidly to 20 μs or more one day prior to conjunction. The rapidity with which conditions change just before conjunction is indicated by the expanded plots in Figure 5. In the six days before conjunction the path displacement is rapidly decreasing from about 15 solar radii, and scintillation and refractive effects are increasing rapidly and are becoming measurable. Magnetoionic effects should begin to be observed in this time period. It is clear that the six days before and after conjunction will be a very critical period in the radio propagation experiment. The earth-probe range rate from which the expected Doppler frequency can be determined and the angle between the probe earth-line and probe sun-line which has some bearing on the possibility of using directive antennas on the probe, have also been calculated (Figures 6, 7).

These same calculations were repeated for a direct injection launch such that the earth's orbital velocity is augmented by the satellite excess-velocity vector and the satellite travels in an antisolar direction in an orbit having aphelion at approximately 2 A.U. Interestingly enough, for the same launch velocity, conjunction is achieved in the same one-year period (Figure 8) but without producing alternate regions of constant path length

EARTH-PROBE ORBITS

DIRECT INJECTION

Figure 8

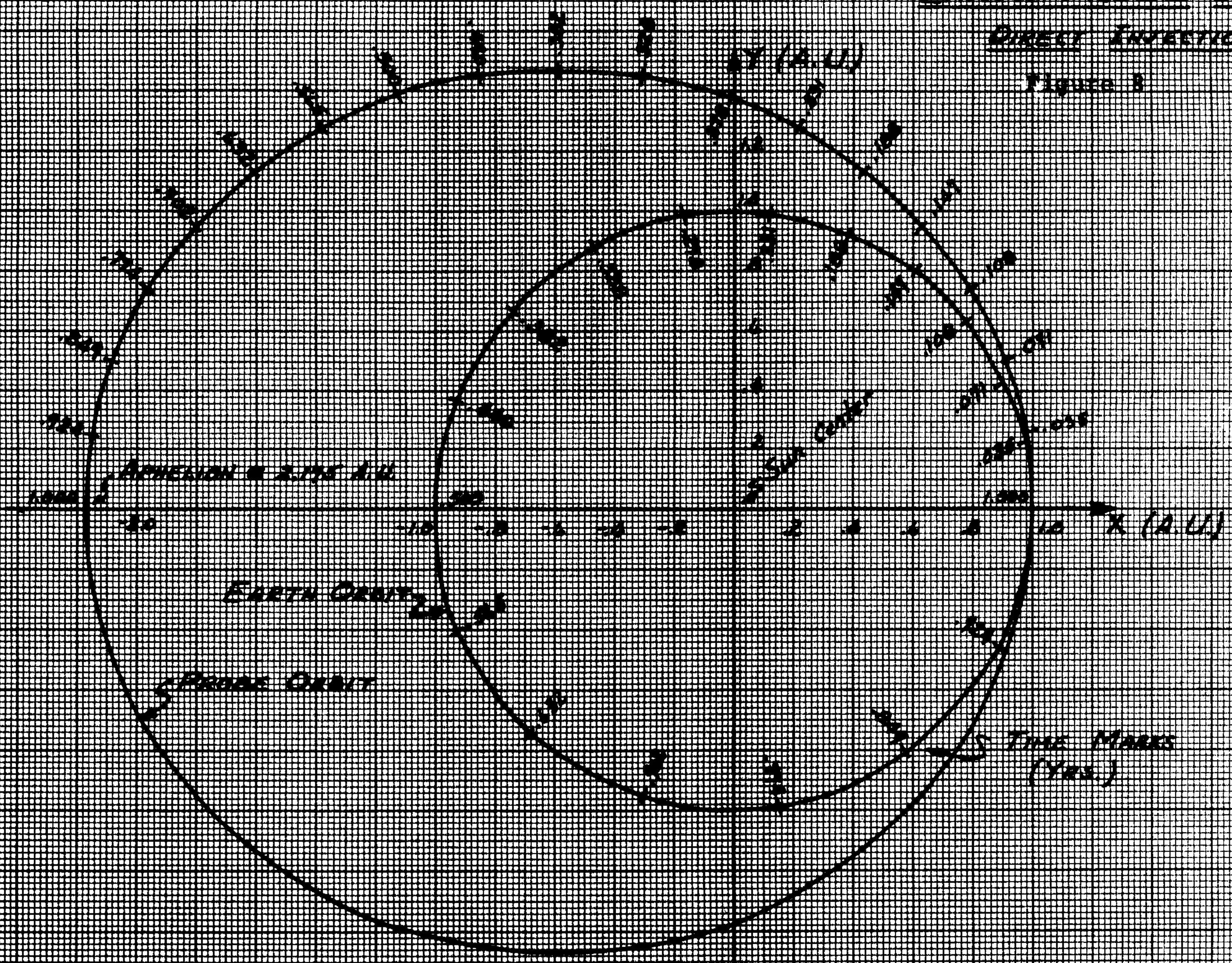

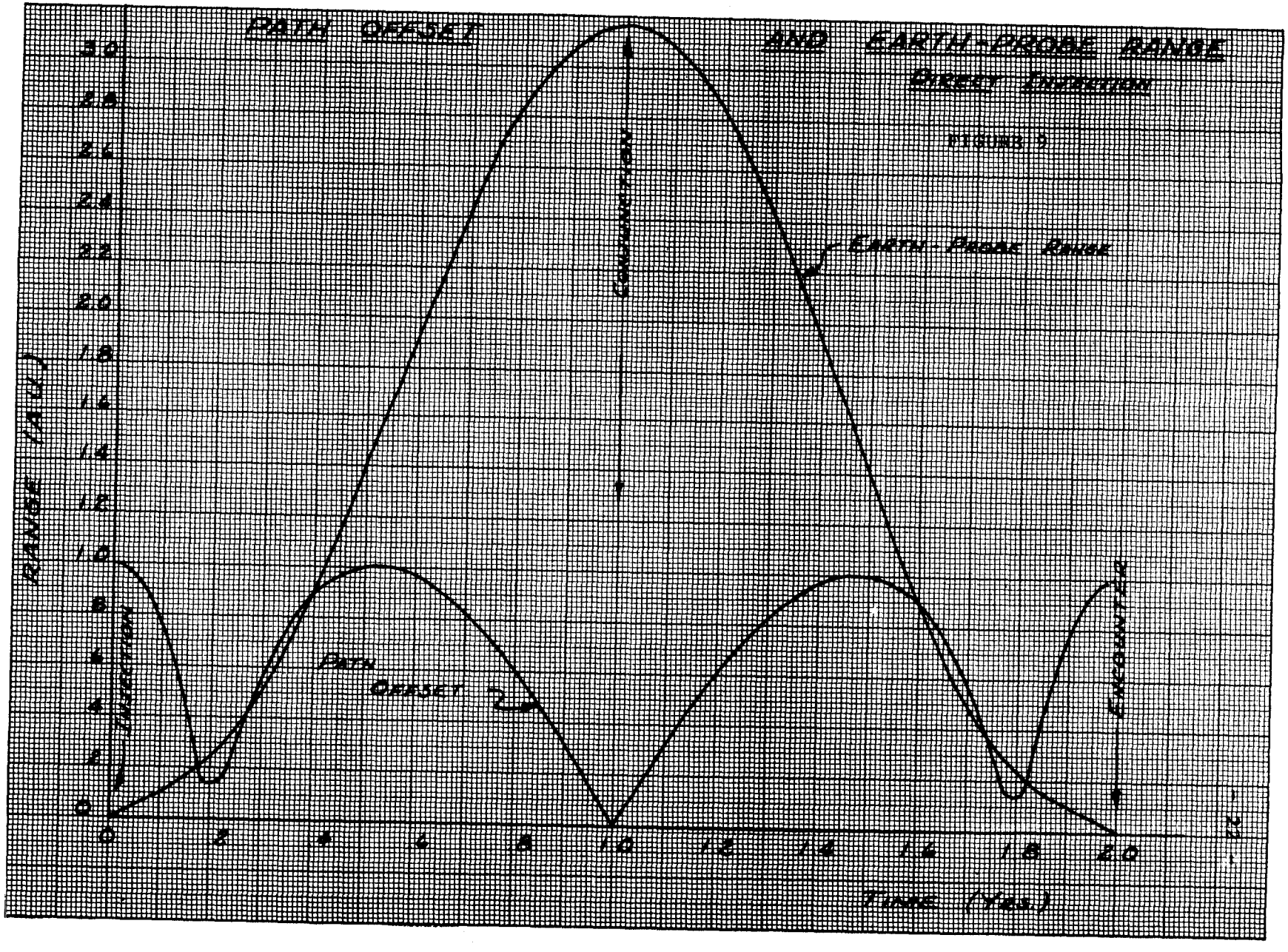
PATH OFFSET AND EARTH-PROBE RANGE
DIRECT INJECTION
FIGURE 5
EARTH-PROBE RANGE
PATH OFFSET
RANGE (R)
TIME (Yrs.)
0
2
4
6
8
10
12
14
16
18
20
22
24
26
28
30

EARTH - PROBE RANGE RATE

DIRECT INJECTION

FIGURE 10

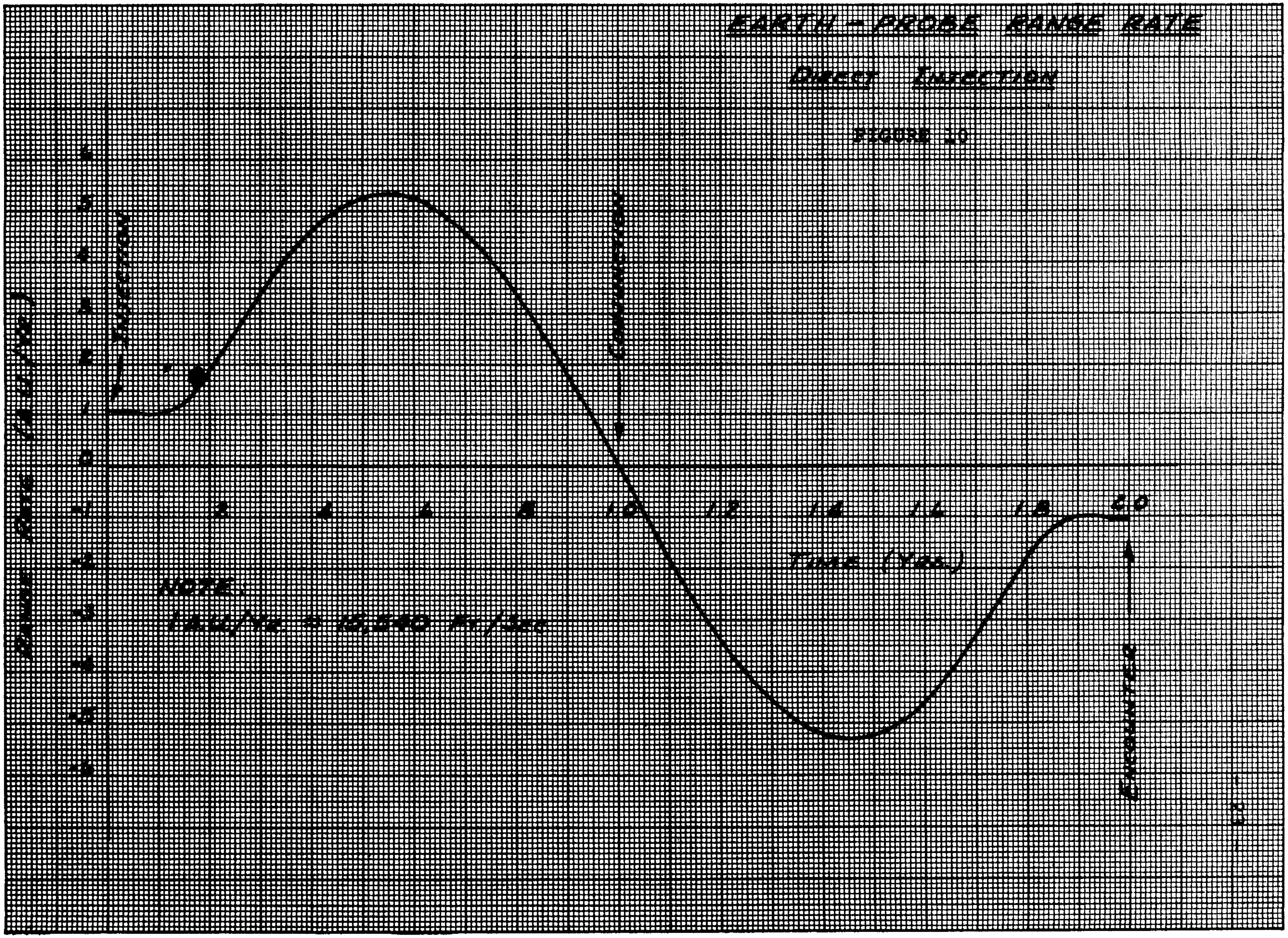

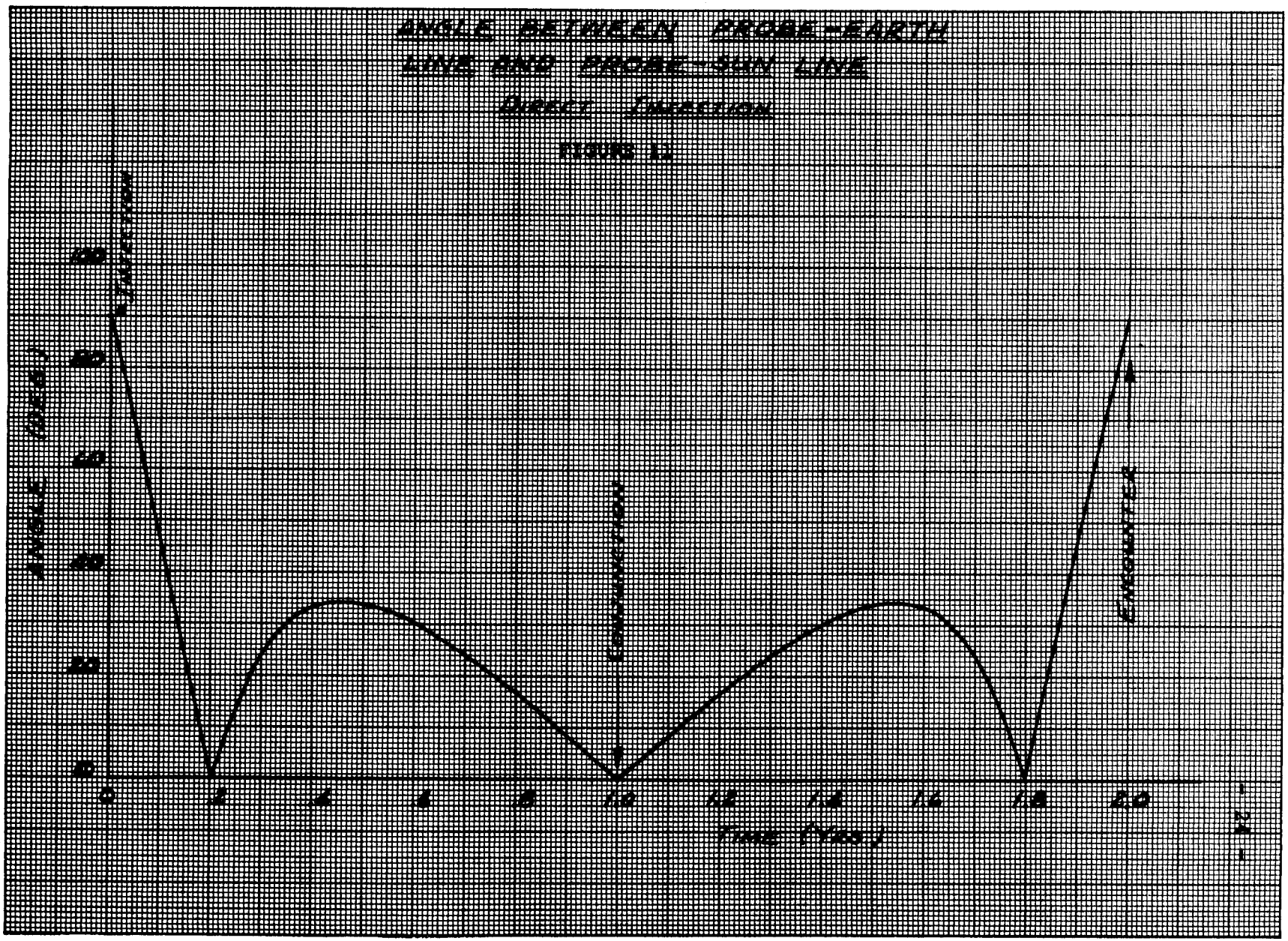
ANGLE BETWEEN PROBE-EARTH LINE AND PROBE-SUN LINE
DIRECT EMISSION
FIGURE 12
ANGLE (DEGREES)
40
20
0
2
4
6
8
10
12
14
16
18
20
TIME (HRS.)
DIRECTION OF SUN
DIRECTION OF EARTH

and constant displacement (Figures 9, 10, 11) as in the retrograde injection case. The path has a maximum length of 3.2 A.U. so that more power is required for transmission. It does not appear to be an attractive orbit to use to study the region between three and 100 solar radii, but for studying the interplanetary regions beyond 0.5 A.U. this orbit has very great attractions and might be an appropriate future Sunblazer mission.

D. Coronal Scattering

Radio waves propagating through a turbulent refractive medium are scattered in angle about the median ray. The total energy is constant but distributed in angle in accordance with the law:

$$p(\phi) \propto \varepsilon^{-(\frac{\phi}{\phi_o})^2} \qquad [12]$$

[Chandrasekar, 1952; Fejer, 1954] ϕ_o is a measure of the half-width of the angular scintillation spectrum and for ray paths through the solar corona has been shown to follow the law:

$$\phi_o = \frac{K\lambda^2}{r^n} \qquad [13]$$

[Hewish, 1963; Erickson, 1964; Högbom, 1960] where r is the displacement of the path in solar radii from the solar center, and λ is the wavelength in meters. The λ^2 dependence seems well established on theoretical grounds and is also confirmed experimentally. On the other hand, the magnitude of K and the r-dependence have only been determined empirically and vary somewhat between observers. In a recent summary Erickson finds

that n = 2 and that K = 50 where the units of ϕ_o are minutes of arc. An earlier determination [Hewish, 1955, 1963] found that $1.3 < n < 2.2$ and $K \sim 11$. Since both K and n must depend on the magnitude and scale size of the electron density fluctuations in the corona at the time of measurement, it is not surprising that some variability in these coefficients should be observed over portions of the solar cycle and confirms the desirability for observing the coronal densities at different stages of solar activity. The refraction angle or mean angle through which the ray is bent has been computed for various electron density profiles. For a ray through the Allen-Baumbach corona, the refractive bending is:

$$\theta = \frac{76\lambda^2}{r^3} \text{ minutes of arc} \qquad [14]$$

Scintillation and refractive effects for a 100 MC wave propagated through the corona have been extrapolated from the results of Hewish [1963] (Figure 12). At 10 solar radii the expected half-width scintillation is 3' and the refraction 1'; at five solar radii the two quantities differ only slightly, at 6' and 4' respectively; and at 2.5 solar radii the refraction is greater, the values being 19' and 34', respectively. Thus a 100 MC signal received by a half-degree beamwidth antenna (D $\sim$ 1,000 feet) would be attenuated appreciably by scattering losses for paths within 2.5 solar radii of the sun. As the ratio of the mean square scintillation angle to the beam width approaches

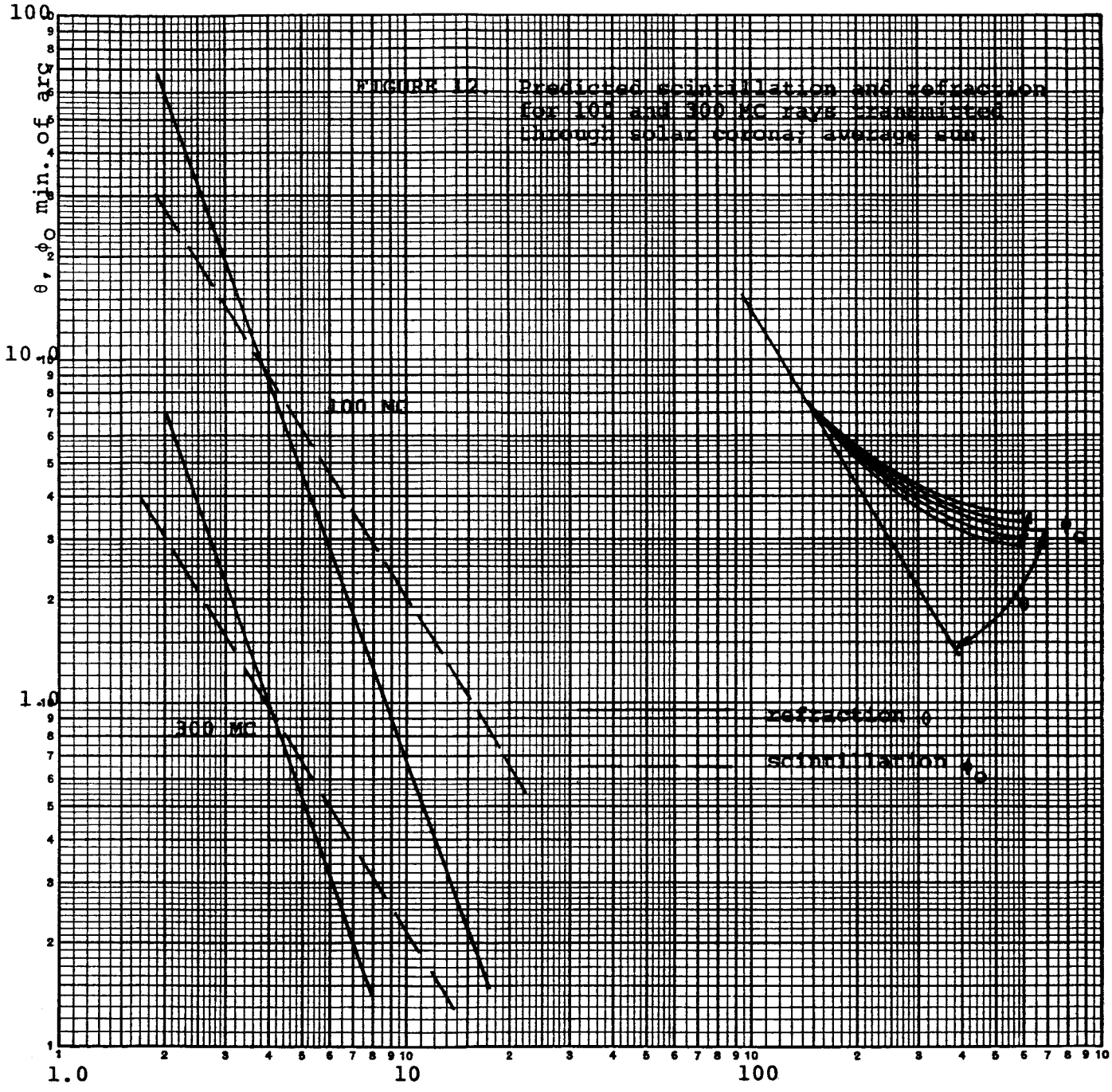

FIGURE 12. Predicted scintillation and refraction for 100 and 300 MC rays transmitted through solar corona; average sun.

unity, an increasing fraction of the transmitted wave is scattered out of the antenna beam pointed in a fixed direction. If one had an antenna such as a rapidly adjustable, phased array, capable of very rapid pointing, this effective attenuation could be reduced by tracking the instantaneous angle of arrival of the radiowave. This would be possible if the fluctuation times were long compared to the beam-pointing and signal-integration times. These scintillation fluctuation times have not yet been measured, but would appear to depend on the size and velocity distributions of the plasma clouds crossing the transmission path.

If we assume a scale size in the 1,000 to 10,000 km range for the plasma fluctuations and an outwardly moving velocity in the 100 to 1,000 km per second range, crossing times of one to 100 seconds are implied and suggest comparable fluctuation times in the angle of arrival of the ray on earth which rates are slow enough to be measurable.

For a simple model in which the scattering is isotropic, Chandrasekar [1952] finds that:

$$\overline{\phi_o^2} = \overline{2L^2/\ell^2} \qquad [15]$$

where L is the rms fluctuation in path length and ℓ is the scale size or distance over which the plasma fluctuations are correlated. Unfortunately the isotropic model does not quite apply to scattering in the corona. Evidence exists of anisotropic scattering produced by a filamentary distribution of plasma along generally radial magnetic field lines [Hewish, 1958; Högbom, 1960; Slee, 1961].

However, to the extent that the model does apply to scattering either along or orthogonal to the field lines, Eq. [15] implies that a simultaneous measurement of the fluctuation spectra of angle and time of arrival permit a unique determination of the scale of turbulence to be made in the inner corona where essentially all of the scattering is produced. For example, inhomogeneities 1,000 to 1,000 km in size will give rise to readily measurable 10 to 100 microsecond fluctuations in arrival time for 100 MC signals transmitted on a path displaced by two solar radii from the solar center. At 10 solar radii, the corresponding fluctuations in time of arrival vary from 0.3 μs to 3 μs and would be difficult to measure using the 20 μs resolving power presently planned for the radio propagation experiment.

E. Magnetoionic Effects

It is known that the polarization of a plane electromagnetic wave, propagating through a plasma in the presence of a magnetic field having a component in the direction of propagation, will undergo a rotation given by:

$$\Delta\psi = \frac{2.34 \cdot 10^6}{f^2} \oint n_e \vec{B} \cdot \vec{ds} \text{ radians} \qquad [16]$$

where n_e is the number of electrons/cm^3 and B is flux density in gauss. The relationship holds when the transmitted frequency is much greater than either the plasma frequency or the electron cyclotron frequency of the medium. Both of these conditions obtain for frequencies 100 MC or greater transmitted through the corona.

The Faraday rotation is one manifestation of the slightly different phase velocities possessed by the right and left hand circularly polarized components into which the plane wave can be resolved. If the number of rotations is large enough, the velocity differences can be observed as the differences in time of arrival of the same signal propagated in the ordinary and extraordinary mode. This difference time, $\Delta\tau_{ox}$, is related to the Faraday rotation by the simple expression:

$$\Delta\tau_{ox} = \frac{\Delta\psi}{\pi f} = \frac{2.39 \cdot 10^6}{\pi_{f^3}} \oint n\vec{B} \cdot d\vec{s} \qquad [17]$$

The Faraday rotation observation in situations where either the electron density or the magnetic field configuration is known provides a sensitive means for estimating the missing variable, but the rate must be sufficiently low so that cycles can be counted accurately over the period of the observations.

In the Sunblazer experiment where short daily periods (hours) of observing time are contemplated over the lifetime of the experiment, it might be quite difficult to count accurately the rotation cycles unless the rotation rates were consistent enough from day to day to provide some continuity to the measurement. The pulse-splitting measurement, on the other hand, can offer unique information in one observation and appears to represent a better technique to employ for the observations of the magnetoionic effects in the inner corona. One can derive an expression for the expected Faraday rotation as a function of path displacement for an assumed

general magnetic field configuration in a manner similar to that employed to estimate the expected signal delays. Thus, for the total rotation along a semi-infinite transmission path, assuming that both the electron density and the general field in the plane of the ecliptic (roughly the solar equatorial plane) have cylindrical symmetry, we can write:

$$\Delta\psi = \frac{2.34 \cdot 10^6}{f^2} \int_{\rho}^{\infty} \frac{n(r) \cdot B_{\ell}(r)\ r\ dr}{\sqrt{r^2 - \rho^2}} \qquad [18]$$

If B(r) is resolvable into radial and tangential components, then the component of B along the path is:

$$B_{\ell} = B_r(r) \frac{\sqrt{r^2 - \rho^2}}{r}\ ds + B_{\theta}(r) \frac{\rho}{r}\ ds \qquad [19]$$

$$= B_r(r)\ dr + B_{\theta}(r) \frac{\rho}{\sqrt{\rho^2 - r^2}}\ dr \qquad [20]$$

Hence:

$$\Delta\psi = \frac{2.39 \cdot 10^6}{f} \int_{\rho}^{\infty} n(r)\left[B_r(r) + B_{\theta}(r) \frac{\rho}{\sqrt{\rho^2 - r^2}} dr\right] \qquad [21]$$

$$= \Delta\psi_r + \Delta\psi_{\theta} \qquad [22]$$

where:

$$\Delta\psi_r = \frac{k_1}{f^2} \int_{\rho}^{\infty} n\ B_r\ dr \qquad [23]$$

and $$\Delta\psi_\theta = \frac{k_1}{f^2} \int_\rho^\infty nB_\theta \frac{\rho}{\sqrt{\rho^2 - r^2}} dr \quad [24]$$

As before, these have Abel transforms, such that:

$$\frac{k_1}{f^2} n \cdot B_r = \frac{d}{d\rho} \Delta\psi_r \quad [25]$$

$$\frac{k_1}{f^2} n \cdot B_\theta = -\frac{r}{\pi} \frac{d}{dr} \int_r^\infty \frac{\Delta\psi_\theta}{\sqrt{\rho^2 - r^2}} d\rho \quad [26]$$

For a symmetrical transmission path, B_r is oppositely directed on either side of the point of closest approach, so that:

$$\Delta\psi_r \Big|_{-\infty}^{\infty} = 0 \quad [27]$$

$$\Delta\psi_\theta \Big|_{-\infty}^{\infty} = 2\Delta\psi_\theta \quad [28]$$

To the extent that the general field of the sun can be said to have radial and azimuthal components which are cylindrically symmetric, the Sunblazer Faraday rotation measurement will provide a measurement of the product of the electron density and the azimuthal component of the general field in the region $3 < r_\odot < 10$.

Since n(r) profile is independently measured in the delay experiment, an expression for the field distribution $B_\theta(r)$ can

then be uniquely determined provided, of course, that the fluctuations of the total rotation are small and $\Delta\psi$ can be considered a reasonably well-behaved function. The extent to which one can predict $\Delta\psi$ or $\Delta\tau_{ox}$ is dependent on the availability of good estimates for the general magnetic field of the sun.

Unfortunately, rather spotty data exist on this point. The situation was recently reviewed [Severny, 1964], and it appears that the nature of the general solar field since its initial observation in 1908 remains largely a mystery. The simple model suggested by the observation of coronal rays, to the effect that the general field is a dipole-like field with poles generally aligned with the axis of rotation of the sun and having a magnitude of a few gauss at the poles in the photosphere, is still plausible. The polarity of the field appears to have reversed three times since 1930. Spectroscopic measurements made by observing the Zeeman splitting of emission lines indicate localized fields at sun spots as high as several thousand gauss.

The magnetic field well away from the photosphere may be expected to be a field trapped within the heavily ionized plasma of the solar wind and is expected to be progressively more disordered at greater distances from the sun [Parker, 1961; Mustel, 1964]. Recent measurements by direct probe show the field generally to follow a spiral direction near the earth and to have a magnitude of the order of 10^{-5} gauss.

Strong components orthogonal to the ecliptic plane are observed as well as field directions pointed both into and away

from the sun [Ness, 1964, 1965]. It is difficult in the presence of all these fragmentary bits of information to postulate any simple model for the general solar field, but if one exists it seems likely that in the region within 20 solar radii it is generally radial in direction as revealed by Taurus occultation measurements and as determined by the bulk velocity of the solar wind. It probably has a value of from one to 10 gauss at one solar radius and probably varies as $\frac{1}{r_2}$ to the extent that there is any appreciable concentration of the solar plasma in the ecliptic plane [Parker, 1964].

If the field is assumed to be radial and symmetrical with a magnitude described by:

$$H(r) = \frac{H_0}{r^2} \qquad [29]$$

then the Faraday rotation produced on one side of the path bisector would be equal and opposite to that produced on the other half of the path, and the net rotation would be zero. It is useful, however, to have an estimate for the uncompensated Faraday rotation on half the path. The half-path rotation can be directly measured using the path geometry (Figure 2B) obtained four months after launch. Using the expression for electron density, Eq. [2], and for radial field, Eq. [29], in equation [30] we find:

$$\frac{\Delta\psi}{2} = \frac{k}{f^2} \int_{\rho}^{\infty} \left(\frac{10^8}{r^6} + \frac{10^6}{r^2}\right) \frac{H_o}{r^2}\, dr = \frac{kH_o}{f^2} \left[\frac{10^8}{7r^7} + \frac{10^6}{3r^3}\right] \qquad [30]$$

$\frac{\Delta\psi}{2}$ will be greater (Figure 13) than the angle through which the

polarization angle will be rotated by the earth's ionosphere when $r < 10$. To a certain extent the estimate given by $(\frac{\Delta\psi}{2})$ is a maximum estimate since the oppositely direct rotation on the other half of the transmission path and the effects of alternately directed radial fields trapped in the solar plasma will, on the average, reduce the total rotation. The fluctuations in rotation, however, might be expected to be a modest fraction of $\frac{\Delta\psi}{2}$.

It is therefore hard to say with certainty that a consistent rotation or a consistent pulse splitting will be observed in the Sunblazer experiment. One can only say that the fluctuating character of the Faraday rotation and the extent to which there is any consistent pulse splitting will shed some general light on the gross nature of the general magnetic field in the corona within 10 solar radii. Any appreciable skewness of the field will result in an increased longitudinal component along the transmission path and a larger average Faraday rotation, Eq. [28].

F. Attenuation

An electromagnetic wave propagating through an isotropic plasma will be attenuated by an amount:

$$\kappa = \frac{\nu(\frac{f_\rho}{f})^2}{c\sqrt{1 - (f_\rho/f)^2}} \qquad [31]$$

where ν is the effective electron-ion collision frequency and f_ρ is the plasma frequency [Ginsburg, 1964]. The dependence of collision frequency on parameters such as electron density, electron

and ion temperatures, various cross sections, is a complicated one, but to a good approximation (within 5 percent) in the inner corona.

$$\nu_{eff} \simeq 42 \times 10^{-6} \, NT^{-3/2} \qquad [32]$$

where N is in units of meters^{-3}.

In the case where $f >> f_\rho$ we then find:

$$\kappa \simeq \frac{\nu}{c} \frac{f_\rho^2}{f^2} \qquad [33]$$

$$\kappa \simeq 1.13 \cdot 10^{-11} \frac{N^2 T^{-3/2}}{f^2} \qquad [34]$$

Taking $T = 10^6$°K and $f = 10^8$cps, then:

$$\kappa_{100 \text{ mc}} \simeq 10^2 \times 10^{-36} \text{ nepers/meter} \qquad [35]$$

The total attenuation along a ray path through an isothermal corona is then:

$$A(\rho) = 2 \int_\rho^\infty \kappa \, ds \qquad [36]$$

$$= 2K_a \int_\rho^\infty \frac{\nu(r) n(r) r \, dr}{\sqrt{r^2 - \rho^2}} \qquad [37]$$

where K_a is a constant. As in the case of the delay and rotation integrals, this is also an Abel integral which has a unique transform:

$$K_a \, \nu(r) n(r) = - \frac{1}{\pi} \frac{d}{dr} \int_r^\infty \frac{r}{\rho} \frac{A(\rho) d(\rho)}{\sqrt{\rho^2 - r^2}} \qquad [38]$$

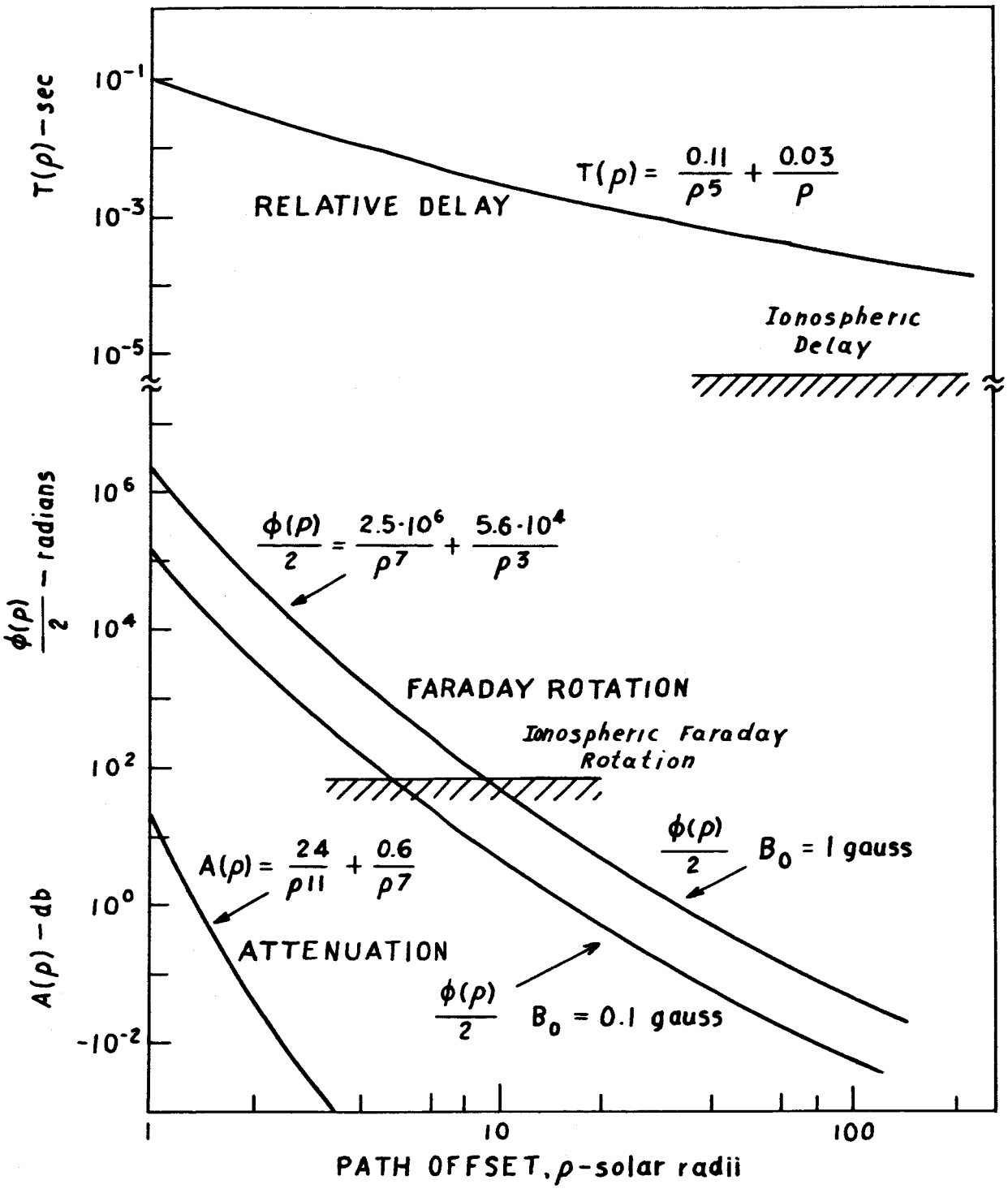

FIGURE 13. 100 MC propagation along infinite path through extended solar corona (group delay, attenuation, and Faraday rotation as function of path offset)

so that a measurement of $A(\rho)$ and the separate (delay) determination of $n(r)$ would permit a unique determination of collision frequency.

Using the Allen-Baumbach electron density in Eq. [1] and assuming an isothermal corona with $T_e = 10^{6}°K$, we find:

$$A(\rho) = \left[\frac{24}{\rho^{11}} + \frac{0.6}{\rho^{7}} + \frac{0.005}{\rho^{3}}\right] \text{ decibels at 100 MC} \qquad [39]$$

The attenuation falls off very rapidly with path displacement. For $\rho = 2$, $A(\rho)$ is only 0.02 db so that for the Sunblazer propagation experiment where $\rho > 3$, $A(\rho)$ would in all likelihood not be measurable.

G. Choice of Frequency

The group velocity for a wave packet propagating through an ionized medium with no magnetic field present [Spitzer, 1962] is given by:

$$\left(\frac{v_g}{c}\right)^2 = 1 - \left(\frac{f_p}{f}\right)^2 \qquad [40]$$

where the plasma frequency $f_p^2 = 81 \cdot 10^6$ n and n is the number of electrons per cm^3.

The relative delay between signal propagation on frequencies f_1 and f_2 through this plasma is then:

$$T = \oint \left(\frac{1}{v_{g_2}} - \frac{1}{v_{g_2}}\right) ds \qquad [41]$$

$$T = \frac{1}{c} \oint \left(\frac{1}{\sqrt{1 - (f_p/f_1)^2}} - \frac{1}{\sqrt{1 - (f_p/f_2)}} \right) ds \qquad [42]$$

for

$$f_2 > f_1 > 3f_p$$

$$T \approx \frac{1}{c} \oint \frac{f_p^2}{2f_1^2} \left[1 - \left(\frac{f_1}{f_2}\right)^2\right] \quad ds \qquad [43]$$

or

$$T = \frac{1.35 \cdot 10^{-3} N}{f_1^2} \left[1 - \left(\frac{f_1}{f}\right)^2\right] \text{ seconds} \qquad [44]$$

where $N = \int nds$ is the total number of electrons per square centimeter along the transmission path.

This simple relationship between delay and integrated electron density is valid so long as $f > 3f_p$. On the other hand, if f_1 is very much greater than f_p, the sensitivity of the measurement is poor since a large number of electrons then only produce a modest delay. The best choice seems to be to make f_1 slightly larger than the plasma frequency of the innermost region of the corona through which the transmitted ray is to penetrate. At 1.5 solar radii the plasma frequency is approximately 40 MC which suggests a frequency near 100 MC for f_1.

The choice of the reference frequency f_2 is not critical so long as it is sufficiently greater than f_1 to make the quantity $\left[1 - \left(\frac{f_1}{f_2}\right)^2\right]$ as close to unity as possible.

The choice of a 300 MC reference carrier gives a relative delay 0.89 percent of that achievable with an infinitely high

reference and seems a good choice to make for reasons of implementation.

Since the number of Faraday rotations also varies as $\frac{1}{[f]^2}$, the choice of the lowest possible frequency for f_1 will enhance magnetoionic propagation effects and improve opportunities to observe gross features of the solar magnetic field. The half-width of the scintillation spectrum is also proportional to the square of the wavelength, so that the lower frequencies provide greater sensitivity for scale-of-turbulence measurements.

While the choice of the 100 MC probing frequency appears to permit penetration to about 3.5 solar radii, it might also be desirable, payload weight permitting, to transmit a 40 MC signal which would enhance delay, scintillation, and Faraday rotation effects but would only permit measurement to about six solar radii.

H. Minimum Path Displacement

The minimum observable displacement of the transmitted ray from the photosphere depends on other factors as well as the magnitude and scale size of electron density fluctuations in the inner corona. Of particular importance is the directivity of the receiving antenna that is used to observe the transmitted signals. For example, the desire to reduce the solar noise contribution to the overall receiver noise temperature makes it important to keep the antenna pointed at least a half-beamwidth away from the photosphere. For a fairly broad beam, quite large

minimum penetration distances are then implied. For example, to limit solar noise a 4° beamwidth antenna could only be pointed within about 2° of the photosphere, and the minimum path displacement would then be 9 solar radii. Conversely, if the beamwidth is excessively narrow, then the scattering produced by inhomogeneities in the corona will cause an effective attenuation of the signal when the scintillation spectrum approaches the antenna beamwidth.

By using the empirical expression for the half-width of the scattered distribution:

$$\phi_o = K \frac{\lambda^2}{R^n} \qquad [45]$$

where

$$\bar{n} = 2$$

$$1.7 < n < 2.5$$

$$K \simeq 50 \text{ minutes at solar minimum}$$

$$K \simeq 100 \text{ minutes at maximum}$$

and equating this to the half-width of the antenna beam $(\frac{\lambda}{D})$ where the beam is assumed to be a fan beam with its narrow dimension generally along a solar radius, we find:

$$\frac{(57.3)(60)}{2} \left(\frac{\lambda}{D}\right) = K \frac{\lambda^2}{R^2} \qquad [46]$$

From this the maximum usable aperture is:

$$D_{max} = 34.4 \frac{R^2}{\lambda} \text{ at solar minimum}$$

$$= 17.2 \frac{R^2}{\lambda} \text{ at solar maximum}$$

The minimum usable aperture is obtained from the constraint that the antenna cannot be pointed within a half-beamwidth (approximately) of the photosphere without incurring a solar noise penalty. Thus:

$$\frac{(57.3)(60)}{2}\left(\frac{\lambda}{D}\right) = 15\ (R - 1) \qquad [47]$$

or

$$D_{min} = 115\ \frac{\lambda}{(R-1)} \qquad [48]$$

These two limiting apertures define an allowable operating region (Figure 14) and the convergence of the two limits defines the minimum path displacement for which observations can be made. Thus:

$$\frac{115}{(R-1)} = 34.4\ \frac{R^2}{\lambda} \qquad [49]$$

or

$$3.34\lambda^2 = R_{min}^2\ (R_{min} - 1) \text{ at solar minimum} \qquad [50]$$

$$6.68\lambda^2 = R_{min}^2\ (R_{min} - 1) \text{ at solar maximum} \qquad [51]$$

Under average conditions for $R > 3$, these reduce to:

$$R_{min} \simeq 1.69\lambda^{2/3} \qquad [52]$$

and the corresponding aperture is then:

$$D_{opt} \simeq 70\lambda^{1/3} \text{ meters} \qquad [53]$$

From these we find the approximate values for R_{min} and D given in Table II.

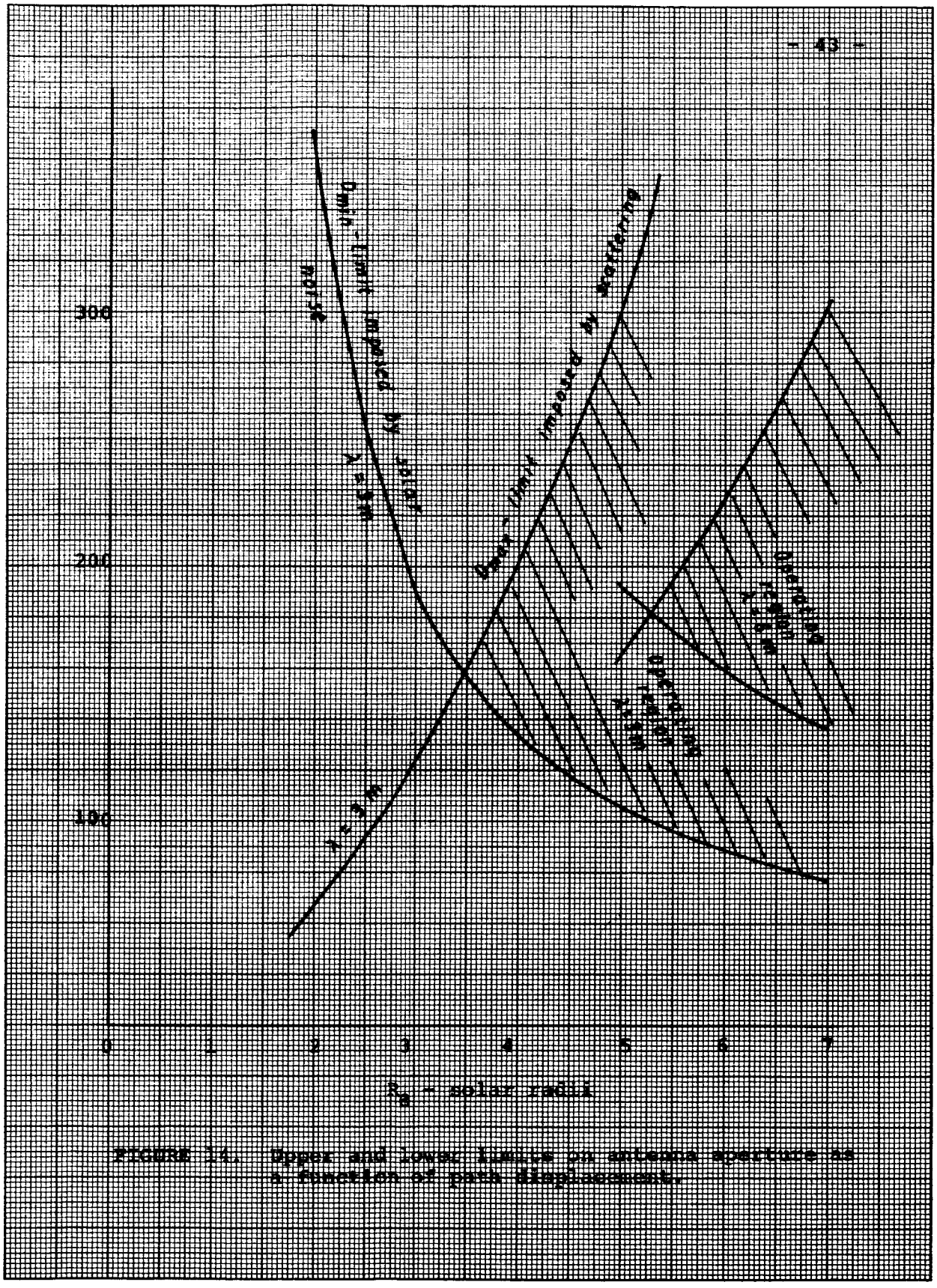

FIGURE 14. Upper and lower limits on antenna spectrum as a function of path displacement.

TABLE II

f	λ	R_{min}	D_{opt}	$\Delta\theta = \frac{\lambda}{D}$
200 MC	1.5 m	2.54 solar radii	114 m	45 min. of arc
100	3.0	3.52	137	75
50	6.0	5.75	145	140

The data suggest that the best beamwidth to use for close-in observations of 100 MC signals is approximately one degree, which would allow observation of ray paths displaced from the solar center by 3 - 4 solar radii. The foregoing calculations are based on a very simple model, and a more careful computation using the actual brightness distributions of the corona for the particular frequencies concerned would probably show a slightly greater radius of closest approach.

I. Path Loss Computations

The required transmitter power on the spacecraft may be calculated from the usual path-loss equations. The received power P_R is given by:

$$P_R = P_t G_t \frac{1}{4\pi R^2} A \qquad [54]$$

where P_t is the transmitted power, G_t is the gain of the spacecraft antenna, R is the transmission distance, and A is the effective area of the receiving antenna.

For a half-wave antenna on the spacecraft, $G_t = \frac{\pi}{2}$, the maximum range r_{max} = 1.5 A.U. For a circular paraboloid $A = \frac{\pi}{4}d^2$ where d is the antenna diameter in mm. The noise power is given by the familiar kt Δf where $k = 1.38 \times 10^{-23}$ watts/° K per cycle. The noise temperature will be determined by the galactic background at the observing frequency. If we avoid observations at the time the earth-sun line is in the plane of the galaxy (which means December occultations are excluded), the mean galactic background at 100 MC is about 700° K. For our computations we assume $T = 10^{3}$° K.

The received signal-to-noise ratio is then given by:

$$\frac{P_R}{P_N} = \left(\frac{J}{10}\right)\left(\frac{A}{705}\right) \qquad [55]$$

or, for a circular aperture,

$$\frac{P_R}{P_N} = \left(\frac{J}{10}\right)\left(\frac{D}{30}\right)^2 \qquad [56]$$

where $J = \frac{P_t}{\Delta f}$ is the energy per pulse in joules and D is the antenna diameter in meters. Thus, a 10-joule pulse having a peak power of one kw and a pulse width of 10 ms would be received on a 30-meter dish with unity signal-to-noise ratio. A 300-meter dish (approximately the Arecibo dish) would provide a 20 db signal-to-noise ratio on one 10-joule pulse. The large-diameter dish is desirable both for the directivity that permits observations close to the sun and also for improved detection sensitivity.

The 140 m aperture shown to be optimum for minimum path displacement provides a 13 db dignal-to-noise ratio on a 10-joule pulse and would seem to promise acceptable performance on both counts.

J. Modulation

It was indicated earlier that pulse energies of the order of 10 joules or greater are required, and for practical reasons with the spacecraft peak power limited to about one kw, pulse widths of the order of 10 ms result. This is not sufficiently narrow to give the time resolution desired for most of the propagation measurements of interest so that coding within this long pulse must be employed. We have elected to use a triply-folded, 11-bit Barker code to obtain the necessary compression ratio [Barker, 1953]. The N-bit Barker code has the property, as shown in Figure 15, that the peak of its autocorrelation function is N and that its remaining side lobes never exceed unity. The individual pulses will be identified by a phase reversal modulation and will be 20μs in duration. An 11-bit code would then be 220μs long. A second encoding (fold) made up of these 220μs groups or their out-of-phase replicas would then give a second code 11 times 220μs or 2.42 ms in duration. Then finally a third fold will give a final pulse width of 26 ms. The virtue of using the triply-folded Barker code as opposed to employing simply 1320 randomly phase-reversed pulses is that the folded code permits some simplicity in instrumentation and some gradual loss in resolution in the

a) The Eleven-bit Barker Code

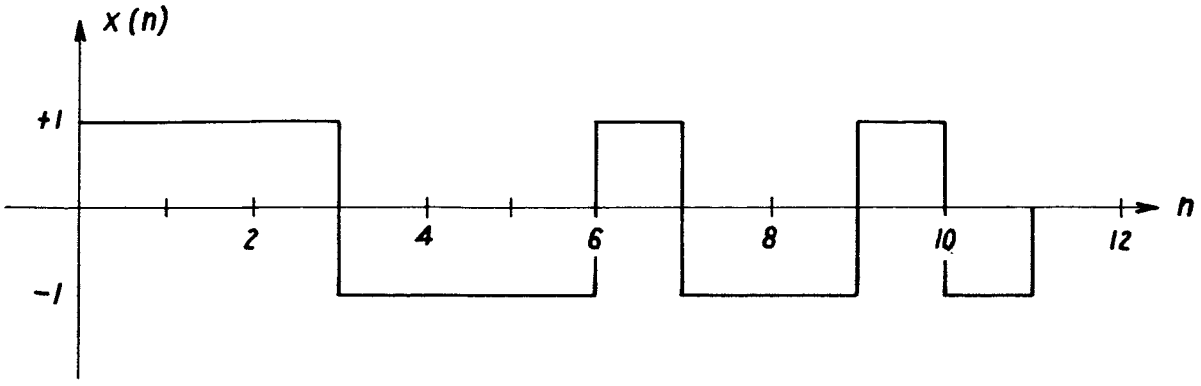

b) The Corresponding Autocorrelation Function

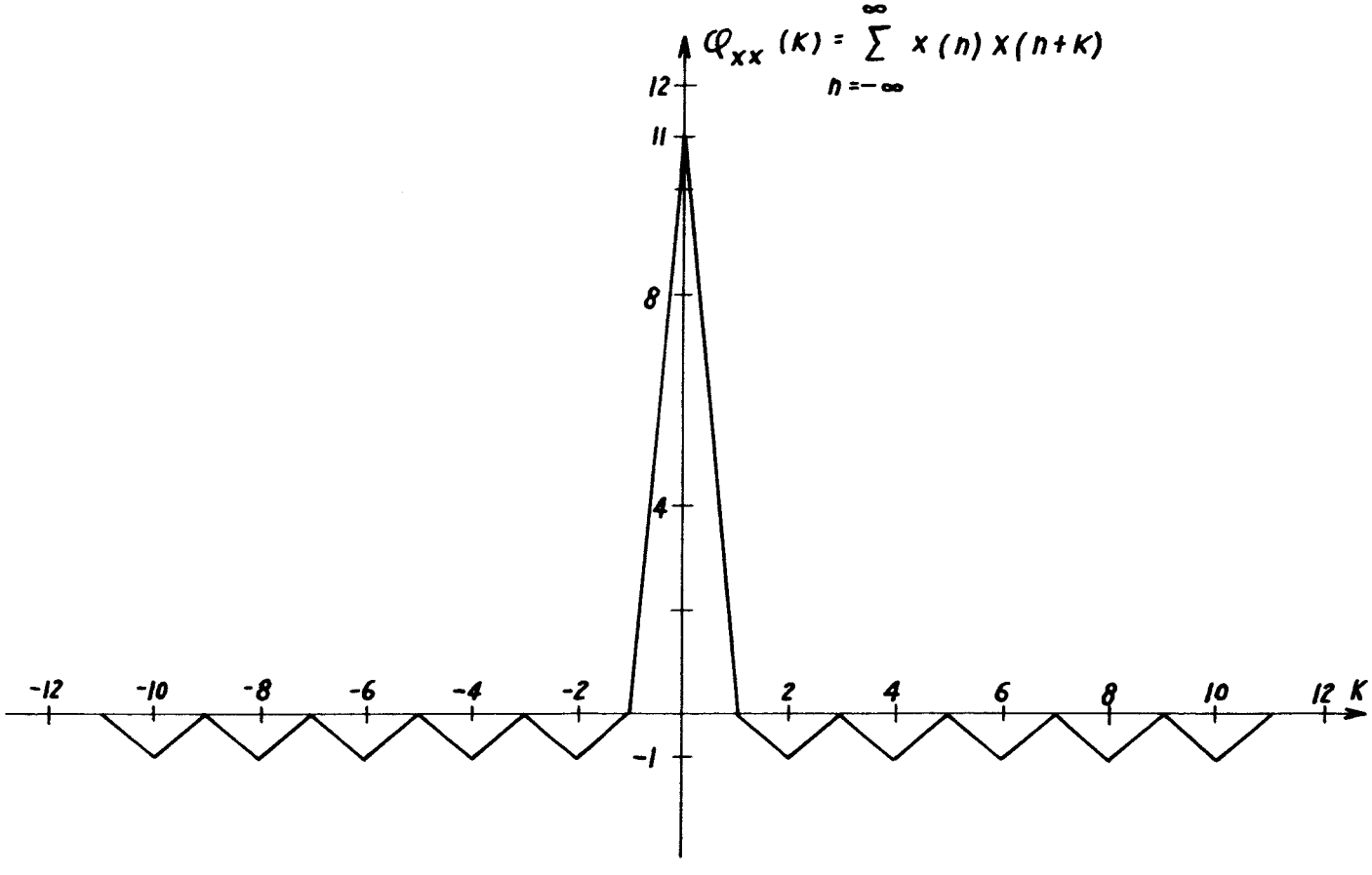

FIGURE 15

presence of serious delay distortion in the interplanetary medium. That is, if the coherent bandwidth of the medium is not sufficient to transmit a 20μs pulse, it might sustain a 220 ms pulse and the next highest fold might be satisfactorily detected, and so on. The more random codes do not have this feature. When the elementary pulses can no longer be resolved, the code in general fails. In transmitting through an unknown medium as we are, the graceful death feature of the Barker code seems a very desirable one.

REFERENCES

Allen, C. W.: "Interpretation of Electron Densities from Coronal Brightness," Monthly Notices, Royal Astron. Soc., 106, 137, 1947.

Barker, R. H.: "Group Synchronizing of Binary Digital Systems," Characteristics of Transmission Channels, in Communication Theory, pp. 273-287, Academic Press, 1953.

Baumbach, S.: "Strahlung, Ergiebigkeit und Elektronendichte der Sonnenkorona," Astronomische Nachrichten, 263, pp. 121-134, 1937.

Brandt, J. C., R. W. Michie, and J. P. Cassinelli: "Coronal Temperatures, Energy Deposition, and the Solar Wind," Icarus 4, pp. 19-36, 1965.

Bridge, H. S., A. Egidi, A. J. Lazarus, E. F. Lyon, L. Jacobson: Proc. Int. Space Sci. Symp. 5, Florence, 1964.

Chandrasekar, S.: "A Statistical Basis for the Theory of Stellar Scintillation," Monthly Notices, Royal Astron. Soc. 112, #5, pp. 475-483, 1952.

Erickson, W. C.: "Radio-Wave Scattering Properties of the Solar Corona," Astro. Phys. J. 139, pp. 1290-1311, 1964.

Fejer, J. A.: "The Diffraction of Waves in Passing through An Irregular Refracting Medium," Royal Soc. Proc. 220A, #143, pp. 455-471, 1953.

Ginzburg, V. L.: Propagation of Electromagnetic Waves in Plasmas, Addison-Wesley Press, pp. 39-53, 1964.

Harrington, J. V.: "First-Order Analysis of Sunblazer Orbits," M.I.T., Center for Space Research TN-64-1, July 1964.

Hewish, A.: "The Irregular Structure of the Outer Regions of the Solar Corona," Proc. Royal Soc. 228A, pp. 238-251, 1955.

Hewish, A.: "The Scattering of Radio Waves in the Solar Corona," Monthly Notices, Royal Astron. Soc. 118, #6, pp. 534-546, 1958.

Hewish, A. and J. D. Wyndham: "The Solar Corona in Interplanetary Space," Royal Astro. Soc. 126, #5, pp. 469-487, 1963.

Högbom, J. A.: "The Structure and Magnetic Field of the Solar Corona," Roy. Astro. Soc. 120, #6, pp. 530-539, 1960.

Mustel, E.: "Quasi-Stationary Emission of Gases from the Sun," Space Sci. Rev. 3, pp. 139-231, 1964.

Ness, N. F. and J. M. Wilcox: Phys. Rev. Letters 13, p. 46, 1964.

Ness, N. F. and J. M. Wilcox: "Sector Structure of the Quiet Interplanetary Magnetic Field," Goddard Space Flight Center #X-612-65-157, April 1965 (submitted to Science).

Parker, E. N.: "Solar Wind," Space Astrophysics; Sec. II, The Theory, McGraw-Hill Book Co., pp. 164-168, 1961.

Severny, A.: "Solar Magnetic Fields," Space Sci. Rev. 3, pp. 451-486, 1964.

Slee, O. B.: "Observations of the Solar Corona Out to 100 Solar Radii," Roy. Astro. Soc. 123, #3, pp. 223-231, 1961.

Spitzer, L. A.: Physics of Fully Ionized Gases, Interscience, 2nd ed., pp. 52-54, 1962.

van de Hulst, H. C.: "The Electron Density of the Solar Corona," Bull. Astro. Insts. of Netherlands, XI, #410, pp. 135-160, Feb. 2, 1950.

Vitkevich, V. V.: Paris Symposium on Radio Astronomy, Stanford University Press, R. N. Bracewell, ed., p. 275, 1959.

Wild, J. P., K. V. Sheridan and A. A. Neylan: "An Investigation of the Speed of the Solar Disturbances Responsible for Type III Radio Bursts," Australian J. Phys. 12, #4, pp. 369-398, 1959.